MASSACHUSETTS INSTITUTE OF TECHNOLOGY
LINCOLN LABORATORY

REGISTRATION ERRORS IN A NETTED AIR SURVEILLANCE SYSTEM

W. L. FISCHER
C. E. MUEHE
Group 43

A. G. CAMERON
Group 41

TECHNICAL NOTE 1980-40

2 SEPTEMBER 1980

LEXINGTON MASSACHUSETTS

ABSTRACT

Today's tactical military air surveillance radars generally operate in a stand-alone configuration. The many performance improvements that result when data from multiple radars of this type are merged have made such netted operations an attractive goal for many years. A major obstacle to achieving this goal has traditionally been the difficulty associated with the registration of multisensor data, the expression of the data in a common coordinate system free from errors due to site uncertainty, antenna orientation, and improper alignment.

This report presents the results of a modest effort to develop a self-registration procedure by which multiple radar sensors operating in consort each calculate the errors in their data by comparing it with data from the remainder of the system and then uses the information to upgrade performance. The technique has been tested with experimental data and appears quite capable of improving system performance, measured in terms of residual inter-site bias errors, by almost a factor of one hundred.

CONTENTS

I. INTRODUCTION

Since an air surveillance radar was first developed prior to World War II, military planners have given much attention to the netting of individual sensors; the combining of data from multiple sensors to provide a universal picture of the overall air situation. Attempts at such integration have traditionally met with limited success.

There are many reasons why such integration is desirable, indeed necessary in some situations. As weapon system technology advances and reaction times diminish, many of these are becoming critical.

A. Quality of Coverage

Individual radar sensors are limited, both in the volume of airspace (especially at low altitudes) they can search and in the quality of the air track data they can form, particularly with respect to tracking maneuvering aircraft through rapidly varying flight profiles. Effective integration of multisensor data could fill coverage gaps and could more rapidly discriminate between maneuvers and surveillance errors.

B. Reliability

When a stand-alone radar site is attacked successfully all users of its output data are effectively denied information. An integrated system whose output is shared among all users would produce data whose quality would degrade only gradually as individual sites were eliminated.

C. Coordination of Identity Data

An integrated air surveillance system would necessarily employ a common track data base to which additional information, particularly information regarding friend or foe identity, could be readily added no matter how derived. A single positive identification of a particular target could serve to provide all data users with its identity status for the duration of its lifetime within the system, thus reducing the need for a highly reliable, new, IFF system.

D. Increased Reliance on Automation

The quality of sensor data available from today's radar equipment, especially in ECM situations, is such that automated processing of that data frequently yields only marginal performance and human intervention is necessary to determine which tracks are valid, which targets represent actual aircraft, and so forth. For many years attempts have been made to develop systems that are less manpower intensive, both by improving radar data quality and by improving the sophistication of the processing algorithms. The capability to operate on data derived from multiple sites could lead to significant improvements in automated system performance and result in a far higher degree of automation using today's radar systems than can be obtained when those systems are operated in the present stand-alone mode.

E. ECM Resistance

An integrated system would be naturally resistant to ECM since the sectors of individual radar sensors that are disrupted by jamming would effectively be filled in by other radars whose geometry, relative to the ECM source, would be different. In addition, the communication links and the ability to operate from a common data base that form the basis of the integrated system would readily support a unified approach to emission control and other ECCM techniques.

F. Integration with Other Systems

Other systems which establish or employ position/location information (e.g., JTIDS, PLRS, inertial navigators) could readily be integrated with the netted radar surveillance system since its common-grid coordinate system and the registration process essential to the establishment of that system would readily support such integration.

These attributes have been recognized as advantageous in many applications for several years, and numerous attempts have been made to achieve them by integration of multiple radar sensors. Some of these have been successful, some have not, depending mainly on the position accuracy required from the integrated system. In general, integrated systems in which required accuracy is less than

a few miles have not been readily achievable. Studies of past history in this area suggest that the reason for this is inadequate ability to perform registration on the multiple input sources; that is, to align them to a common coordinate system. Performance in this area has been traditionally limited by data processing capability; the several coordinate conversion "shortcuts" necessary to perform processing within the capabilities of available digital processors resulted in worst-case accuracies of several miles. With the advent of powerful and inexpensive real-time computers it is appropriate to reexamine the registration process to determine whether it can result in significant improvements in accuracy. This report does that and concludes that accuracy improvements of more than two orders of magnitude are realizable with presently available technology. A highly precise registration algorithm is developed and verified with experimental data. This algorithm could form the basis of an automated self-registration system that would make feasible the highly accurate integrated air surveillance system of the future.

II. BACKGROUND

The earliest air search radar integration process was developed more than 40 years ago around the "Home Chain" radar sensors which alerted British defenses to German air attack during the Battle of Britain. System accuracies were poor (on the order of several miles), areas of coverage overlap were few (outnumbered by areas of no coverage), and processing/data integration functions were essentially manual. On the other hand, reaction time and vectoring accuracy requirements were sufficiently low so the system proved quite effective.

The development of SAGE in the years following World War II provided the first opportunity to merge automatic computing technology with radar data and brought about the first attempts to systematically define and overcome registration problems. The procedures that were developed in SAGE for dealing with data on a single target gathered by multiple radars are essentially those found today in many applications.

- For each volume of airspace a particular sensor is defined as "primary". Other sensors are defined as "secondary", "tertiary", etc.

- Any track within that volume is updated exclusively from data obtained by the primary sensors. If the "quality" of that data (measured in terms of the blip-scan ratio or detection probability) falls below a threshold, input is switched to the secondary sensor, etc.

- At boundaries between volumes for which different sensors provide primary coverage, large discontinuities in tracks occur. Tracking software is programmed to ignore these, and operators are trained to live with them.

This procedure is employed in today's version of SAGE, and is essentially that used in the FAA's enroute radar tracking system, NAS Stage A. (It should be noted that in the FAA's application the procedure more than suffices since aircraft fly prescribed tracks and the measured parameter of most interest is position along track versus time as opposed to the position of the track itself.)

The SAGE procedure for multisensor registration was adopted by the Navy for use in its NTDS (Naval Tactical Data System) which is an automated system for the netting of surveillance data and dissemination of tactical command and control information employed on most larger Naval combatant vessels. The system, of course, involves sensors whose relative positions vary with time, and a more sophisticated registration process is in order. Over the 20 years in which NTDS has been operational the registration software has improved considerably through a sequence of "grid-locking" algorithms and associated algorithms for the alignment of data from multiple radars on the same platforms. Overall registration accuracy is still only on the order of a mile or so, but this would appear sufficient for the purposes of the system as it is currently employed.

Many other attempts at netting radar data have been made in the context of recent, specific systems such as the Army's Missile Minder (TSQ-73), the Air Force's Tactical Air Control System, and the Marine Air Command and Control

System. These systems, for the most part, do not attempt to capitalize on the advantages inherent in multisensor operation; the limited data integration of which they are capable is not considered of paramount importance and, hence, the registration approaches they employ are unsophisticated, in some instances being merely 1980 equivalents of the SAGE approach to registration. With the realization of the advantages to be gained by a more systematic and comprehensive approach to data integration, and the recognition of the vulnerability of essentially stand-alone systems, this situation is slowly changing but no examples of improved registration capabilities consistent with that change are presently apparent in the field.

III. THE INTEGRATED AIR SURVEILLANCE SYSTEM OF THE FUTURE

Present air search/surveillance resources are numerous and varied in capability. Rather than considering the development of a new integrated air surveillance system using a new family of radar sensors, it appears economically attractive to consider the integration of sensors that are presently in use, for the most part in stand-alone operation. These sensors are, for the most part, manual or semi-automated; the quality of the data they produce is generally insufficient to support fully automated track initiation and updating. It is anticipated that the proper form of netting, allowing the sharing of raw target data, will support a higher level of automation than presently realized. Some of the most recent radar equipments, employing fairly sophisticated radar signal processing techniques, provide data of sufficient quality to support this higher degree of automation. The trade-offs between increased netting and this increased processing sophistication as means to accomplishing fully automated tracking are not well understood, but it would seem that material simplification of the basic radar systems could result from proper application of netting and this would offset some of the expenses associated with netted operation.

For a variety of reasons, particularly for minimum cost and to minimize vulnerability to physical attack, the integrated system should be distributed; data merging and processing should be performed at many sites rather than concentrated into a hierarchical structure. It would be appropriate to make those

sites the radars themselves. Suitable addition of digital processing and intercommunication equipments to the radars would suffice to transform present-day sensors into the integrated future system. Consistent with this system architecture, individual sensor sites would "broadcast" data on targets detected and tracks in process, and would employ data received over "broadcasts" from these sensors as well as their own detection data as input to their tracking process.

The definition and development of the appropriate data merging and tracking processes represent a major task; it is clear that proper data registration is an essential prerequisite to these processes. The registration process must transform position data on all targets and tracks to a form suitable for input to each tracking process. To be consistent with the tactical situation, registration should be a continuing process. Upon initial setup of a network of radar sites the registration process should automatically begin to tie the data from those sites together by appropriate adjustment of site parameters based entirely on data derived from targets of opportunity. As more targets with different geometries become processed by the system, the registration process should continually refine its estimates of the biases associated with the individual sites and their error mechanisms. In the case of mobile or readily transportable sites the process should support the tracking of the position of the individual sites and maintain registration throughout movement and reconfiguration activities.

The registration issues addressed in this report represent the first step in the development of such an automated self-registration process; at the heart of any such process is an understanding of the mechanism by which various error sources contribute to total registration error. Section IV covers these in detail.

Given a thorough enumeration of registration error sources, a self-registration algorithm to characterize those sources and correct data for their effects can be developed; this is done in Section V. Some experimental verification of the error model and self-registration algorithm are presented in Section VI. Section VII presents conclusions regarding the pertinence of this

entire topic to an automated integrated surveillance system and recommends additional work in the tracking and surveillance areas needed to bring such a system into being.

IV. SOURCES OF REGISTRATION ERROR

When a single air surveillance sensor is employed for air traffic control purposes only, relative aircraft positions and courses are important. Offsets in range and azimuth which apply equally to all aircraft do not affect performance. When it is desirable to combine two or more overlapping sensor outputs, the situation changes and a variety of error sources must be considered (see Table I). All error sources which would contribute more than a few meters' error in the registration of aircraft reports between two radars are listed in the table and discussed below.

A. Range Errors

There are four types of range errors due to range offset, range clock rate error, propagation, and erroneous slant range correction. Range offset refers to a common increment in range added to all range measurements. The digital range counters found in modern air surveillance radars must be properly zeroed to eliminate range offset by using an accurately surveyed radar target. Once adjusted there is little likelihood of further adjustment even when the radar is moved. Errors in the range clock can produce errors proportional to range. Another range correction is required due to the presence of the troposphere which influences the velocity at which the radar signals propagate. This error is a nonlinear function of aircraft range and height. Appendix A contains a table suitable for use with standard atmospheres and radars located near sea level. From the chart we see that corrections up to over 100 meters are required for long-range aircraft.

Under range error sources we have also listed the obvious error if slant range, as measured by the sensor, is used as a horizontal range. A large error is produced. For instance, at 30° elevation angle the error in horizontal range is about one-quarter of the aircraft's height (about 14 percent of its range). Accurate registration must properly account for aircraft height. How this is accomplished is explained below under coordinate conversions.

TABLE I

SENSOR REGISTRATION, SOURCES OF ERROR

SOURCE	CORRECTIVE MEASURES
RANGE:	
OFFSET	CALIBRATE AT FACTORY
RANGE SCALE	ACCURATE RANGE CLOCK
ATMOSPHERIC CORRECTION	TABULAR CORRECTION
HEIGHT CORRECTION	3D RADAR OR OTHER SOURCES OF HEIGHT INFO (e.g., MODE C)
AZIMUTH:	
OFFSET	NORTH-SEEKING GYRO
ANTENNA TILT	AUTOMATIC TILT MEASURING SYSTEM
TIME:	
OFFSET	TIMING CORRECTIONS PROVIDED BY COMMUNICATIONS SYSTEM
TIME SCALE	ACCURATE CLOCKS
RADAR LOCATION:	
LATITUDE, LONGITUDE, HEIGHT	PLRS, JTIDS, GPS, OR INERTIAL NAVIGATOR
COORDINATE CONVERSION:	ACCURATE ALGORITHMS

B. Azimuth Errors

Errors in azimuth can be caused by incorrect alignment of the radar antenna with the reference azimuth (i.e., north) and by incorrect alignment of its axis of rotation with the local vertical. Azimuth offset error occurs when the radar does not point to true north when its azimuth readout indicates north. North-seeking gyro compasses are available which, when left stationary, will produce a true north reading to 2 milliradians within about four minutes. These would be accurate enough for use with most mobile radars. Alternatively, initial alignment using a magnetic compass could be followed by fine alignment using the self-registration algorithm described later.

Another possible source of azimuth error is antenna tilt. For an ordinary 2D (i.e., non-height finding) rotating sensor with horizontal azimuth bearing two types of antenna tilt can occur. The entire azimuth bearing (and antenna) may be tilted or the azimuth bearing may be level but the electrical axis of the antenna may be tilted. Both tilts produce errors proportional to the tangent of the elevation angle of the target. Bearing tilt will produce error terms proportional to the sine and cosine of the azimuth angle (see error equations in Section V). Azimuth bearing tilt can be minimized either by carefully leveling the azimuth bearing or by using tiltmeter outputs to correct aircraft position reports.

Tilt of the electrical axis above the azimuth bearing should be carefully calibrated at the factory and either removed or used to correct aircraft position reports. Steerable 3D sensors may possess other tilt errors depending on the arrangement of their azimuth, elevation, and traverse axes.

C. Time Errors

Two possible sources of registration error are connected with the timing of aircraft position reports. Various sensors may be offset in time between one another. Also, some sensors may have clocks that run fast or slow. A method for accurately setting the sensor's clock should be devised using the intersensor communications network and accurate crystals should be used in all clocks. For registration accuracy of 10 meters on Mach-2 targets the clocks should be accurate to 20 msec. Present practice is to assume that the time of

the report over the communications link is the time at which the aircraft position was observed. Since more than a 20-msec variation may exist in reporting, a time tag should be incorporated within every position report.

D. Radar Location Errors

Registration errors will also exist if sensor locations are in error. A number of navigation systems can be used to provide accurate location data. These are: the Position Location and Reporting System (PLRS), the Joint Tactical Information Distribution Systems (JTIDS), the Global Positioning System (GPS), and various inertial navigation systems. We will not review each of these navigation systems. All but the last claim to provide location accuracies comparable to the desired 10 meters.

E. Coordinate Conversion Errors

Errors can also result from inaccuracies in the process of converting target coordinates to system coordinates if traditional approximations are made and all corrections are not included. In this regard, choice of the proper coordinate system is important.

Several good reasons can be found for use of an accurate earth-referenced coordinate system. Such a system is also desirable when other locating systems are employed to locate certain targets or components of the air surveillance sensors to serve users also located in geodetic coordinates. For instance, most military aircraft carry inertial navigation systems (INS). When accurately registered in geodetic coordinates the surveillance data could be relayed to friendly aircraft to update their INS. Alternately, the friendly aircraft could report their INS-derived positions for correlation with surveillance sensor data leading to positive identification.

When air defense batteries are located in geodetic coordinates, it is most convenient to supply target coordinates in geodetic coordinates.

Registration in geodetic coordinates allows easy reference to a wider variety of maps and accurate placement of map data on system displays. Airborne radars and direction finders utilize INS for short-term position location. In

order to enter their detection and track data, the system should use geodetic coordinates.

Future navigation systems such as GPS and JTIDS expect accuracies on the order of 10 to 30 meters. The coordinate system and conversion algorithms used in an integrated air surveillance system should match these accuracy numbers. This rules out most of the techniques used for coordinate conversion in present-day, integrated air surveillance systems.

Present-day systems employ stereographic projection (refs. 1-4). The sensor reports are projected onto a plane local to the radar and tangent to a sphere. When received by the master site they are transformed onto the master plane tangent to a sphere at the master site. A second-order transformation is usually employed which is accurate to a few meters (ref. 4) over several hundred miles. Inaccuracies of a kilometer or so are typically introduced however in the stereographic projection to the local plane. Highly accurate, direct conversion of sensor data to geodetic coordinates is fairly simple (see Appendix B) and avoids the necessity for further transformation to each master plane.

The simplicity of data sorting and the absence of any required coordinate conversion are strong factors favoring the reporting of data in geodetic coordinates. Every source or user of data can act independently in receiving and sorting out data which may be useful to him from data being broadcast by other data sources. Thus, a system of sensors and users can grow to as large a network as desired or can contract to a set of autonomous sensors. The use of geodetic coordinates provides a common, well understood language allowing easy communication amongst diverse data sources and users.

The considerations listed above suggest that geodetic coordinates are the best choice in a system of netted air surveillance sensors. Processing complexity has limited their use in the past, but with today's computer capabilities, their innate accuracy justifies the slight additional workload required with a geodetic system.

Since situation displays are generally flat and the world round (nearly), some type of projection must be employed. Where the displayed area is no larger

than one or two hundred miles in extent the Mercator projection is acceptable. A Mercator projection is used for all of the situation figures in this report. Aircraft positions in geodetic coordinates are easily converted to a Mercator projection since lines of constant latitude and longitude are rectangular straight lines and bearing angles are accurately preserved. For displays of very large areas some other projection such as the Lambert conical projection may be desired. To preserve accuracy and maintain maximum convenience all aircraft positions and track projections should be calculated in geodetic coordinates.

V. SELF-REGISTRATION ALGORITHM

Each of the various registration error sources discussed above can be minimized by more careful siting, calibration, etc. An alternative which would appear more attractive in a tactical situation would be a computer algorithm which automatically brings each sensor into registration with the remainder of the network whenever its situation is changed. In any event, an algorithm is required to assess the sensor's alignment with respect to the system.

Upon initial set-up the best estimates of position, north reference, etc., would be fed to the algorithm which would then examine target reports, compare them with those obtained from the remainder of the system, and automatically vary the various registration error correction values to bring the radar into alignment with the rest of the system. The process would use targets of opportunity and would presumably converge on the optimal set of bias error corrections as the number of target detections employed increased and as the entire variety of target/sensor geometries was satisfied. This section discusses such an algorithm, developed at Lincoln Laboratory, which solves automatically for antenna pointing misalignment, range offset and range clock error, time-base differences, and sensor location errors.

While ideally such an algorithm would operate to lock one sensor into an established system of sensors, the one discussed here functions to register two sensors with one another.

In discussing the algorithm it is assumed that the observations have been made by two sensors with overlapping coverage for an extended period of time and

have undergone all necessary preprocessing as described in Appendix C, and that centroided target reports (range, azimuth, altitude, and time) are available from both sensors for each aircraft under consideration. The steps performed by the self-registration algorithm are:

(1) smoothing and coordinating the timing of the target reports from each sensor to generate a smaller set of reports (referred to as "superpoints"),

(2) adjusting the superpoints to account for known biases,

(3) correcting the superpoint ranges for atmospheric refraction,

(4) computing the covariance matrix of the difference of positions as observed by the two radars for each superpoint,

(5) solving for the set of bias components using a maximum likelihood approach, and

(6) estimating the variances of the biases.

Step (5), being iterative, is the least straightforward and most computationally demanding of the six. The steps are discussed in detail in the following paragraphs.

Step 1: Smoothing

Proper bias estimation using data from two sensors observing the same aircraft necessitates target reports which are coincident in time according to the clocks at each sensor and which are also free from non-systematic errors such as might arise from noisy or garbled target reports. Since time errors have been included in the bias model, it is necessary also to have at least first-order approximations to the time derivatives of range and azimuth.

Curve fitting (ref. 10) with fourth-degree orthogonal polynomials was found to satisfy the requirements listed above. Short track segments, lasting about one minute, where chosen for fitting to ensure that aircraft maneuvers could be adequately followed.

A computer program and several associated subroutines were written to accomplish the following individually for range, azimuth, and altitude:

(a) Identify track segments for curve fitting only if the associated time intervals for the two sensors are coincident for at least a specified number of seconds (typically between 10-12 observations).

(b) Compare the mean squared value of the residuals after fitting with a threshold defined for each component based on expected random measurement errors. If the mean squared value exceeds the threshold, then the observation having the largest deviation from the least squares polynomial is discarded and the remaining data is fitted again. Should the mean squared value still be too high, the time interval is skipped over for both sensors and control is passed back to step (a).

(c) Evaluate the polynomials at a common mid-point time. The resulting "superpoint" includes time, range, range rate, azimuth, azimuth rate, and altitude.

Step 2: Initial Correction for Assumed Biases

In some cases approximate bias values may be known beforehand. For example, by plotting altitude during times when the aircraft is performing a steep ascent maneuver, it may be possible to estimate a time offset between two sensors (refer to Figure C-2).

The formulas used to adjust the superpoints for initial, assumed bias values and also for the iterative bias estimation procedure in Step 5 are written below.

SENSOR 1

$$\tilde{\rho}_1 = (\rho_1 + \text{ACTD})\ (1 + \text{RC1})$$

$$\tilde{\theta}_1 = \theta_1 + \text{AZ11} + \tan \eta_1 \cdot (\text{AZ21} + \text{AZ31} \sin\theta_1 + \text{AZ41} \cos\theta_1)$$

SENSOR 2

$$\Delta t = (t + \text{TB12})\ (1 + \text{TB22}) - t$$

$$\tilde{\rho}_2 = (\rho_2 + \text{R2} + \text{ACTD} + \dot{\rho}_2\, \Delta t)\ (1 + \text{RC2})$$

$$\tilde{\theta}_2 = \theta_2 + \text{AZ12} + \dot{\theta}_2\, \Delta t + \tan \eta_2 \cdot (\text{AZ22} + \text{AZ32} \sin\theta_2 + \text{AZ42} \cos\theta_2)$$

$$\tilde{\phi}_2 = \phi_2 + \text{LAT2}$$

$$\tilde{\lambda}_2 = \lambda_2 + \text{LON2}$$

where: the subscripts 1 and 2 refer to sensors 1 and 2,

ρ_1 and ρ_2 are measured aircraft ranges,

θ_1 and θ_2 are measured aircraft azimuths,

η_1 and η_2 are measured aircraft elevation angles,

ϕ_2 and λ_2 are the latitude and longitude of sensor number 2, and

the tilde above certain quantities identify the quantity after correction using the biases, while a dot implies a time derivative.

The biases in the above equations are defined as follows:

ACTD is the sum of the aircraft's transponder time delay measured in range units plus any delay in sensor 1. It is a constant for any one aircraft, but varies from aircraft to aircraft. For skin-painting radars it is a constant.

RC1 and RC2 are range rate errors caused by inaccurate range clock rates,

AZ11 and AZ12 are azimuth offset biases,

AZ21 and AZ22 are tilt biases above the azimuth bearing,

AZ31, AZ41, AZ32 and AZ42 are biases describing the tilt of the azimuth bearing,

TB12 is the time offset bias of sensor 2 relative to sensor 1,

TB22 is the clock rate difference of sensor 2 relative to sensor 1,

R2 is the range offset bias of sensor 2 relative to sensor 1, and

LAT2 and LON2 are the errors in the assumed location of sensor 2.

Step 3: Atmospheric Refraction Correction

Because of delay caused by the earth's atmosphere the observed target range will appear to be greater than it actually is. The refraction correction employed is based on a 20 x 20-element lookup table characterizing an idealized standard atmosphere (see Appendix A). Logarithmic interpolation has been used for values not directly found in the table.

By way of example, the range correction for a target with an elevation angle of 5^{o} at a range of 100 km is approximately 108 m. A few tens of meters is more typical of corrections to target ranges encountered in this study.

For the experimental data described in Section VI no attempt was made to obtain a refraction correction table corresponding to the atmospheric density at the actual sensor locations and mission time since the differences in correction values would be well within the intrinsic measurement error levels of the sensors.

Step 4: Calculation of the Covariance Matrix

As shown in Appendix D, the covariance matrix of the difference in observations from the two sensors is the sum of the measurement error covariance matrices for the sensors. Since the elements of the measurement error covariance matrix are functions of range and azimuth, they should be recalculated anytime range and azimuth are modified in the bias estimation procedure. There are, however, two reasons why this does not appear to be worth the additional burden in computer time. The first is based on the assumption that the biases in the system can be kept small or, at least, can be approximately estimated initially. In that case, the relative change in matrix elements due to small increments in range and azimuth will be correspondingly small. A second reason stems from the fact that the sensor measurement errors are also involved in the covariance matrix and their values are never known exactly.

To summarize - the superpoints are first corrected for known or estimated biases and then adjusted for atmospheric refraction before elements of the difference covariance matrix are computed.

Step 5: Function Minimization

Solving for the bias parameter values which best fit a given set of superpoints from each of two sensors is a problem taken from maximum likelihood theory. As developed more fully in Appendix D, the solution amounts to finding the minimum of a function S which is the sum of the squares of the residual vectors scaled to take into account the orientation of the combined measurement error ellipse. The coordinate transformations from range and azimuth into common geodetic coordinates cause the quantity S to be a non-linear function of the biases.

Several approaches were considered for the minimization. One possibility is to formulate the problem into the familiar matrix equation,

$$A\,x = b$$

where x is the vector of bias components, b is the vector of observed differences in target position and A is the matrix resulting from linearization of the problem by a Taylor expansion. Subroutines are readily available for finding a least-square solution to this problem once the matrix equation is set-up. This approach was ultimately abandoned as more bias components were introduced into the model and the problem of developing analytical expressions for the elements of the A matrix became more involved.

Another standard approach not involving the calculation of derivatives was also investigated. In this algorithm, referred to as the grid search, the function S is minimized in each bias parameter separately. It offers the advantage of straightforward computer programming and did yield useful initial results. However, because it converges very slowly, particularly when the bias parameters are not completely independent, it was not deemed suitable.

A third method was applied which has desirable characteristics of rapid convergence without relying on analytical derivations or the evaluation of derivatives. This algorithm was proposed by Powell (see refs. 5 and 6), and is based on quadratic convergence and some properties of conjugate vectors.

Assuming that M bias components are to be solved for, the algorithm begins with the initial best estimate of the bias vector (the elements of which are the bias components) and a system defined by the M linearly independent coordinate directions. It proceeds as two loop structures (one nested within the other); M iterations of the inner loop, each minimizing S results in the establishment of a new conjugate vector. The function S is then minimized along the new conjugate direction and the outer loop is repeated with the latest estimate of the bias vector replacing the initial best guess.

Each minimization of S along a conjugate direction is accomplished by a two-pass increment and search process. In the first pass the bias vector is incremented until a first approximation to the minimum is found. In the second pass the increment step size is reduced by a factor of 10 and the search is repeated

until a new minimum is detected. As a last step, 3-point parabolic interpolation is employed to solve for the final minimum and the associated value of the bias vector at the minimum.

For true quadratic functions the outer loop is exercised for M iterations before the minimum is reached. This constitutes one pass through the algorithm and is used as the basic performance unit.

The final minimum in S has utility as a measure of the goodness of fit of the bias model for a given set of data. S is a statistical quantity having a chi-squared probability distribution with $\nu = 2N - M - 1$ degrees of freedom. (N is the number of superpoints.) Thus, if the measurement errors in range and azimuth were known and all the biases accounted for, the quantity $S_\nu = S/\nu$ would have an expected value of 1.0 and a variance of $2/\nu$ (at least for large N, see Appendix D, Section E).

Finally, even though S is not a true quadratic function, the Powell algorithm was found to converge fairly rapidly toward a minimum. This is demonstrated in Figure 1 where S_ν has been plotted versus pass number. After only one pass the value of S_ν is seen to decrease from a value of 35.8 to approximately 2.48.

Step 6: Estimating the Variances of the Biases

As pointed out in Appendix D, an estimate of the variance of the bias component can be found from the inverse of the Hessian or curvature matrix H. If ϵ_{ii} is taken as an element on the diagonal of the inverse of H, the relation

$$\sigma^2_{a_i} = \frac{S\ min}{\nu}\ \epsilon_{ii}$$

has been taken as a first-order approximation to the variance in the bias estimate. Note that under ideal conditions the expected value of S/ν is approximately 1 and the variance would depend only on the extent of cross coupling between biases.

VI. EXPERIMENTAL VERIFICATION OF ALGORITHM

Data recorded simultaneously from two sensors was used to exercise the self-registration algorithm. In April 1977, beacon data were recorded using Air Traffic

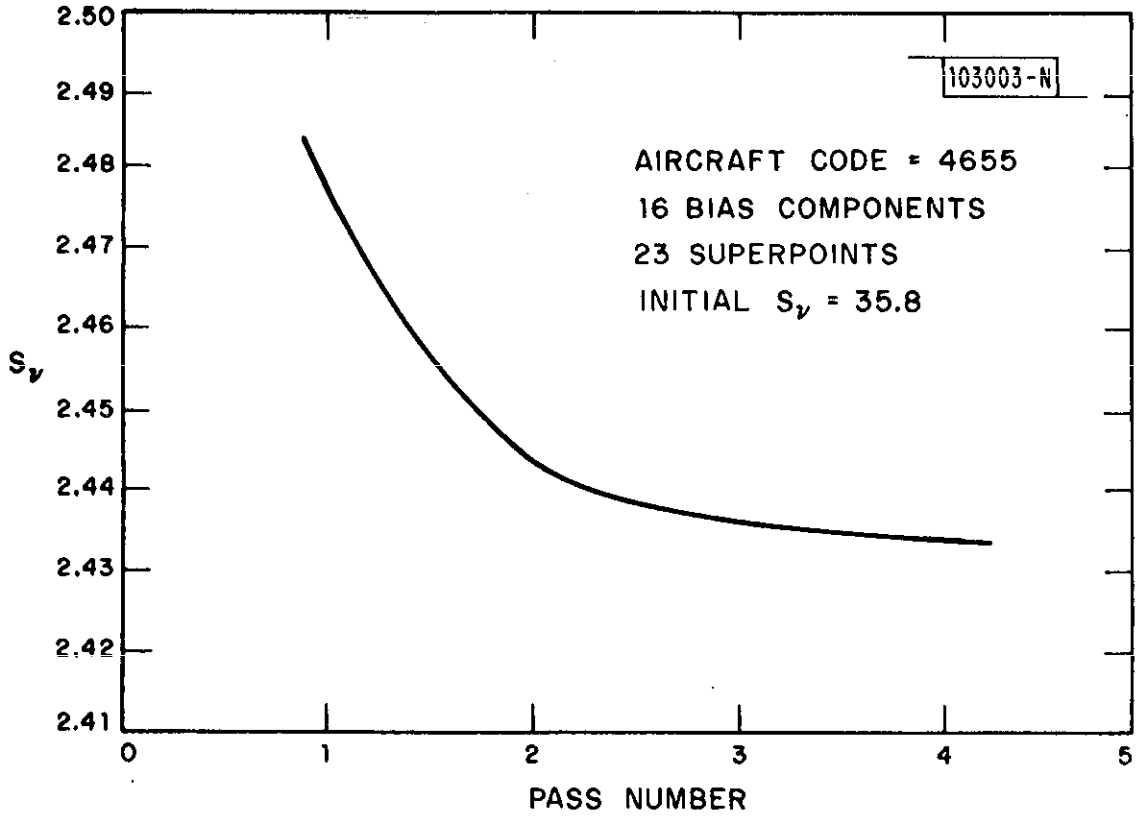

Fig. 1. Minimization using Powell's algorithm.

Control Radar Beacon System (ATCRBS) interrogators. One sensor was located at Lincoln Laboratory, Lexington, Mass., and the other at T.F. Green Airport, Providence, R.I. Figures 2 and 3 are photographs of the two sensors. Each ATCRBS interrogator employed a monopulse antenna for azimuth angle determination. Only four or five interrogations were employed as the antenna scanned by the target. Azimuth was determined on each interrogation and the results were averaged to produce a very accurate azimuth estimate. The sampling rate was once every 4 to 5 sec. for each sensor. Interrogations alternated between Modes A (identity) and C (altitude). The identity code was used to sort out the replies from a particular aircraft. The aircraft's altitude was reported from a barometric altimeter aboard each aircraft to a precision of 100 ft. Data was recorded simultaneously from both sensors over a 35-minute period.

As described in Appendix C, the separate aircraft reports were time tagged. The time had been recorded periodically along with the present azimuth. Target report time was determined by interpolating between azimuth-time reports. Aircraft altitude reports were corrected for the barometric readings at sea level. This involved adding 300 ft to all altitude reports.

Figure 4 shows the paths followed by the aircraft used most often in the analysis which follows. The marked points are the "superpoints". Each aircraft is identified by its code number. The aircraft tracks are plotted in a Mercator projection.

After creating software for the algorithm as outlined in the last section the analysis plan proceeded along the following steps:

1. Verification of the correctness of the procedure through the use of simulated target reports.

2. Comparison of results obtained from different aircraft.

3. Investigation of some approaches toward complete automation of the sensor self-registration problem.

A. Simulation

It became apparent after processing some typical target data that the software could not be adequately tested using real measurements alone. Although

Fig. 2. DABS (Discrete Address Beacon System Experimental Facility) at Lexington, Mass.

Fig. 3. TMF (Transportable Measurements Facility) at Providence, R.I.

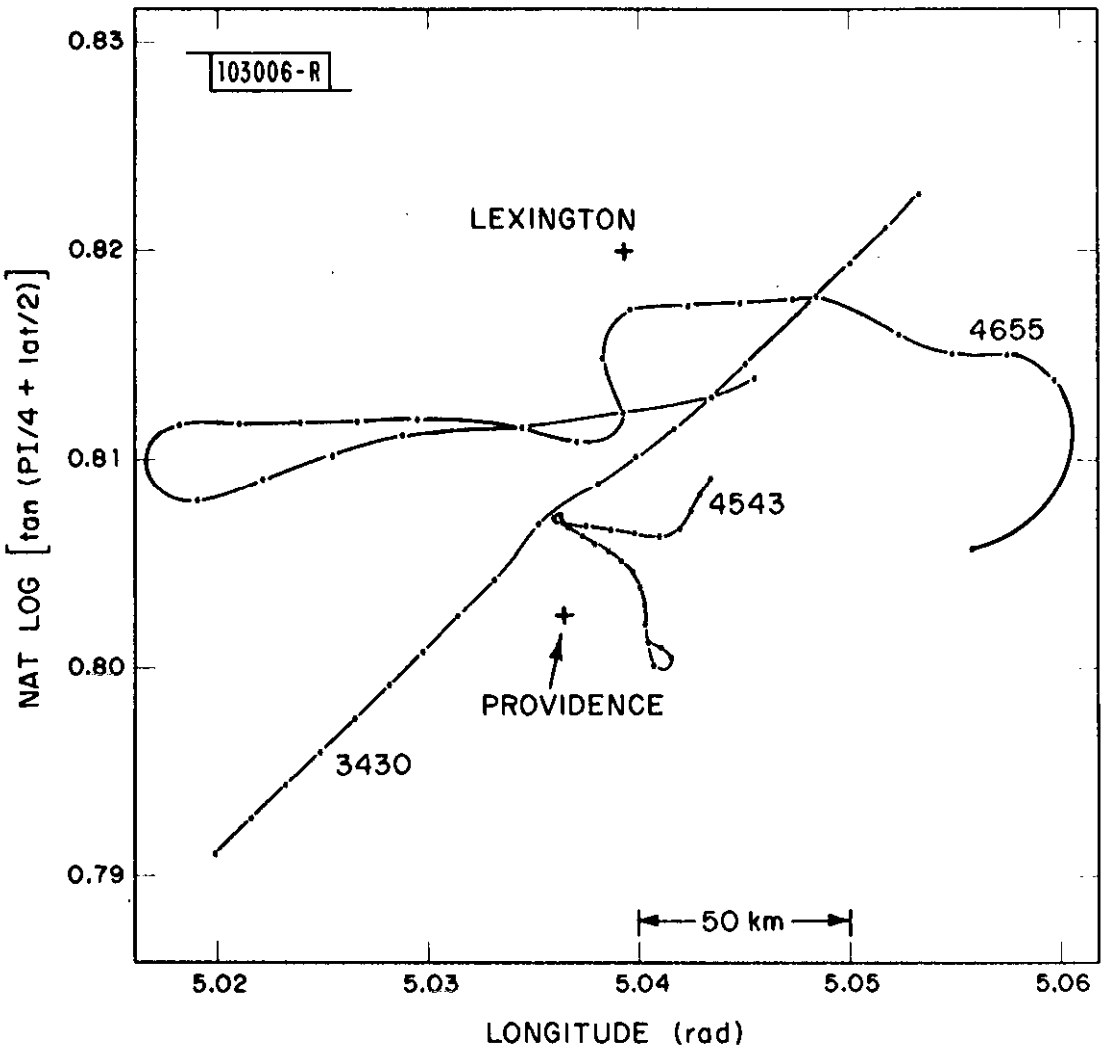

Fig. 4. Mercator projection showing locations and the paths of the aircraft used for analysis.

two large biases were known to exist in the system, little could be surmised about the remaining components.

Simulated data, though not ideal, does at least provide an element of control and, hence, the desired ground truth for general testing purposes. In the interest of making the testing realistic, simulated tracks of target reports were generated from real, Lexington, Mass. data.

Shown in Figure 5 are the steps taken in going from actual Lexington target reports to a file of simulated superpoints for each sensor. The RMS measurement error used for range and azimuth was that assumed for the real data: 10 meters and 0.5 milliradian, respectively. The systematic (bias) error used in the test runs was taken as representative of what could be expected in an operational system. Notice that the Providence reports would agree exactly with the Lexington reports if the noise and bias additions are set to zero.

Using this simulated data, two different algorithm tests were performed. The first was directed at the question, "Given prior knowledge of the presence of a subset of bias components in the observations, how well does the algorithm do in estimating the values of these components?"

To answer this question, Lexington data from target 4655 was used to generate simulated data. Five biases were assumed as in Table II. The self-registration algorithm was applied with the results shown in Figures 6 and 7 and Table II.

TABLE II

SIMULATED TARGET REPORTS

	Known	Computed
AZ11 (rad)	0.003	0.00293
R2 (m)	150	154
AZ12 (rad)	-0.002	-0.00195
TB12 (ms)	-180	-184
ACTD (m)	-100	-110

Assumed Measurement Error

Range RMS = 10 m

Azimuth RMS = 0.0005 rad.

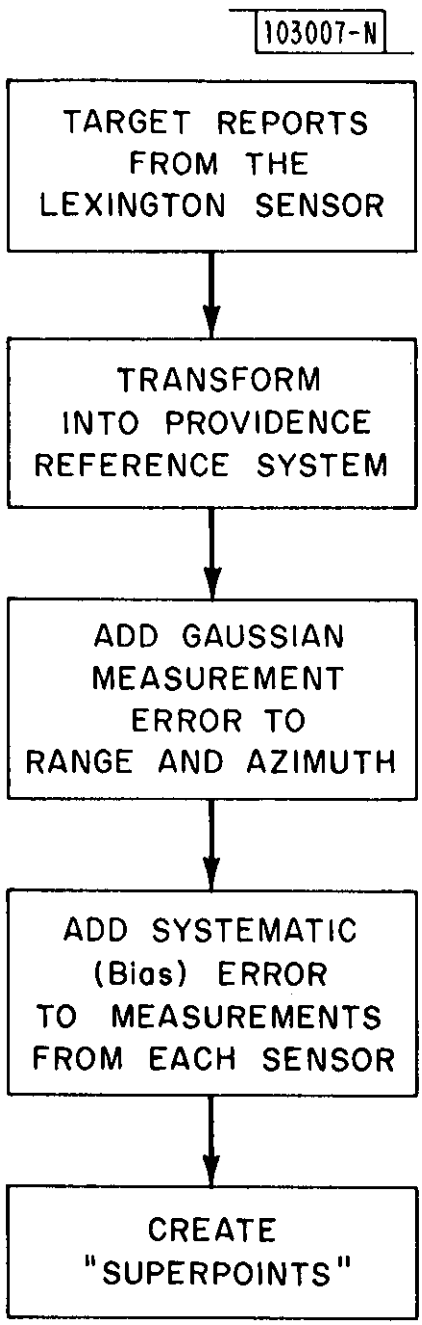

Fig. 5. Generation of simulated target report files.

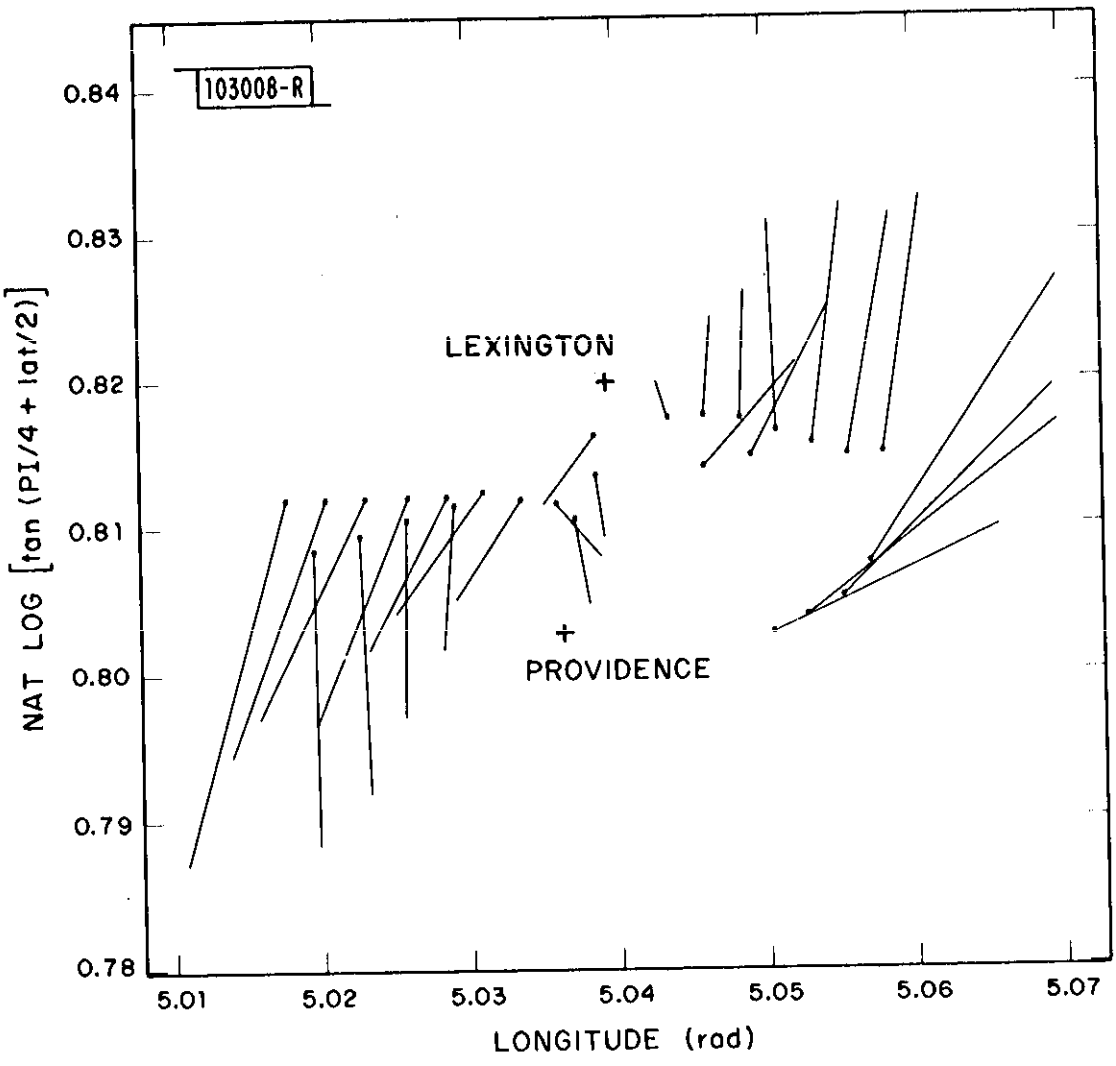

Fig. 6. Superpoints (asterisks) generated from simulated Lexington data and error vectors between sensors magnified 200 times.

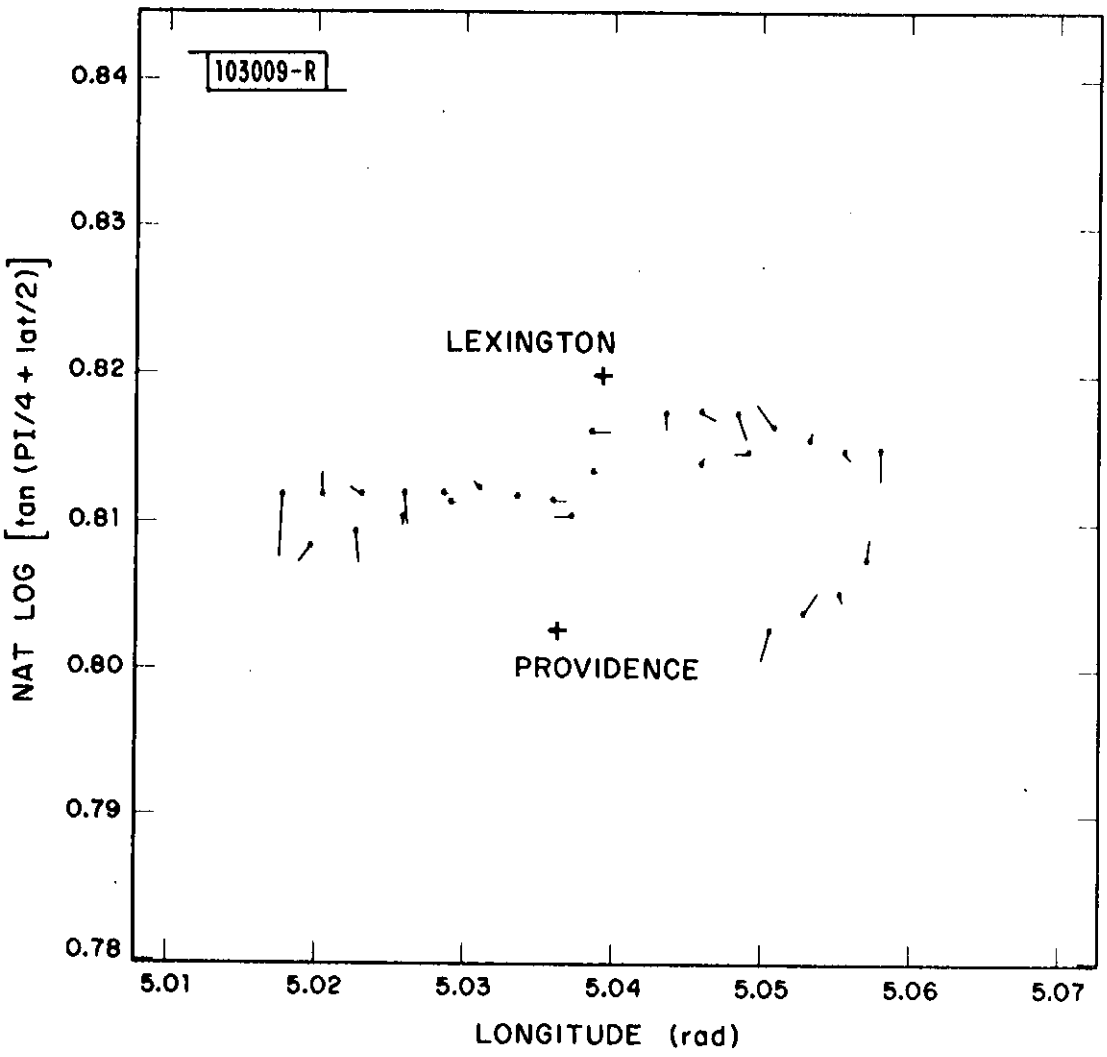

Fig. 7. Simulated superpoints and error vectors after bias removal.

Typical plotted output from one of these test runs is shown in Figure 6. Line segments in the diagram are "error" vectors drawn from Lexington's observed target positions marked by asterisks to those simulated for Providence. The plot is a Mercator projection and for illustration the error vectors are scaled to 200 times actual length.

After only one pass through the algorithm the results in Figure 7 were obtained. The error vectors, now appreciably reduced, are residuals commensurate with the random measurement error introduced into the simulation.

Displayed in Table II are the "known" bias components as compared with values computed by the algorithm. It seems reasonable to conclude from this test that given a priori knowledge of the existence of certain bias components, the algorithm is capable of estimating their values within a relative error of a few percent.

The second level of algorithm testing addressed the more realistic situation in which the presence or absence of individual bias components is not known a priori. In these tests all biases assumed for the model are solved for.

Table III summarizes the output obtained from one of these runs using the same simulated input data of Figure 6. Also tabulated is the standard deviation of the bias estimate computed according to the relationship developed in Appendix D, Section C.

Of particular note in the table are bias components such as AZ21, AZ31, AZ22, AZ32 and AZ42 which have "known" values of zero but have computed values significantly different from zero. As a consequence of solving for all biases in the model, the "known" components with non-zero values are no longer as accurately determined. Some of the discrepancy in reported target position is assigned to the other components. This conclusion is also reinforced by the rather high value of bias standard deviation. For example, the azimuth offset components AZ11 for the Lexington sensor and AZ12 for the Providence sensor have standard deviations nearly an order of magnitude greater than the estimates themselves.

TABLE III

BIAS ESTIMATES FOR SIMULATED DATA

Aircraft Code = 4655

28 Superpoints

Final Value of S_ν = .354

SENSOR	COMPONENT	BIAS ESTIMATE	STANDARD DEVIATION
Lexington, Mass.	RC1	-0.00083	0.00698
	AZ11 (rad)	0.00217	0.033
	AZ21 (rad)	-0.00154	0.0024
	AZ31 (rad)	-0.00141	0.0026
	AZ41 (rad)	-0.00064	0.0026
Providence, R.I.	RC2	-0.00093	0.0066
	R2 (m)	167	62
	AZ12 (rad)	-0.00218	0.032
	AZ22 (rad)	-0.01366	0.008
	AZ32 (rad)	-0.00179	0.0027
	AZ42 (rad)	0.01141	0.006
	TB12 (ms)	-137.3	55
	TB22	0.00004	0.00003
	LAT2 (rad)	0.00001	0.00011
	LON2 (rad)	0.00002	0.00056
	ACTD (m)	-112.6	59

For comparison, similar results using real data are presented in Table IV. Despite the impressive reduction in S_ν from 35.8 down to 2.4 which is a measure of the goodness-of-fit, the high values of standard deviation render the results somewhat questionable. In fact, when other aircraft tracks were used, quite different values for the biases were obtained.

Thus, further insight into the relationships between the bias components was required to avoid generating highly inaccurate bias estimates.

To generate further insight, we examined the Hessian matrix mentioned breifly at the end of Section V and introduced during the development of the bias variance estimates in Appendix D. Because of its relationship to the curvature of S in the space defined by the biases, the Hessian matrix evaluated near the minimum in S can reveal the degree of coupling or correlation among the biases.

Specifically, if h_{ij} are the elements of the Hessian matrix computed by numerical approximation at the minimum in S, then

$$\alpha_{ij} = \frac{h_{ij}}{(h_{ii}\ h_{jj})^{1/2}}$$

defines a coupling coefficient which varies between -1 and +1. A value of α_{ij} near 1 means that an increase or decrease of the i^{th} bias component has the same effect on S as a corresponding change in the j^{th} bias component.

Table V was prepared for the aircraft having an ID code of 4655. It is quite apparent that several biases are tightly coupled for this set of superpoints. Notably high coefficients are found for the pairs: (R2, RC2), (LAT2, ACTD), (AZ12, AZ22), (AZ21, AZ41) and AZ22, AZ42). The results using other sets of superpoints are, in general, different although for certain bias pairs such as (R2, RC2), (AZ11, AZ21), (LAT2, ACTD) and (TB12, TB22) the α_{ij} are consistently high and positive.

Thus, depending on the spatial distribution of an aircraft's superpoints, it may not always be possible to unambiguously estimate those biases contributing to systematic error in the data. Better results will be obtained by not solving for both members of a highly coupled pair. A similar result has been reported by

TABLE IV

BIAS ESTIMATES FOR REAL DATA

Aircraft Code = 4655

23 Superpoints

Assumed Bias: AZ12 = -.2410 (rad)

Final Value of S_ν = 2.4

SENSOR	COMPONENT	BIAS ESTIMATE	STANDARD DEVIATION
Lexington, Mass.	RC1	0.00469	0.0144
	AZ11 (rad)	-0.00344	0.0320
	AZ21 (rad)	-0.00163	0.00730
	AZ31 (rad)	-0.00246	0.00701
	AZ41 (rad	-0.00265	0.00767
Providence, R.I.	RC2	-0.00568	0.0132
	R2 (m)	-425	195
	AZ12 (rad)	-.244	0.0308
	AZ22 (rad)	0.008	0.0217
	AZ32 (rad)	-0.0245	0.00984
	AZ42 (rad)	-0.00331	0.0180
	TB12 (ms)	-124	174
	TB22	-0.0000447	0.000111
	LAT2 (rad)	-0.0000344	0.000193
	LON2 (rad)	-0.0000377	0.000543
	ACTD (m)	76.7	141

TABLE V

COUPLING COEFFICIENTS > 0.5

Aircraft Code = 4655

AZ11			LAT2		
	LON2	.69		AZ31	.60
	AZ31	.83		ACTD	.96
	AZ41	-.70			
RC1			LON2		
	LAT2	.49		AZ21	.69
	AZ32	-.73		AZ41	-.65
	ACTD	.52		AZ22	.73
				AZ42	.69
R2			TB12		
	RC2	.96		TB22	.93
	LAT2	.86			
	AZ31	.69			
	ACTD	.83			
AZ12			AZ21		
	LON2	.72		AZ41	-.94
	AZ22	.93			
	AZ42	.84			
RC2			AZ22		
	LAT2	.76		AZ42	.97
	AZ31	.75			
	ACTD	.69			

Oliver (ref. 7) when using a least-squares procedure to determine the biases in the angular pointing of an antenna.

You will recall that in Table II only a few biases were solved for and that the predicted biases were quite close to the known values. For those superpoints the highest coupling coefficient was 0.79 for the pair (R2, ACTD).

B. Applying Bias Estimates to Several Aircraft

In order to generate bias estimates for application to other aircraft the superpoints shown in Figure 4 were prepared. Three aircraft having identification codes of 4655, 4543 and 3430 were individually processed and then combined into one large data set of 64 superpoints. As can be seen from Figure 4, these superpoints have the reasonably broad geographical distribution desired for bias estimation.

Next, a set of eight bias components was somewhat arbitrarily selected. These were to be the only components solved for and it was required that they be only weakly coupled. The selected components and corresponding coupling coefficients are given in Table VI. Some items require special note: (1) the components ACT1, ACT2 and ACT3 refer to the transponder delay biases for aircraft with codes of 4655, 4543 and 3430, respectively, (2) the matrix is symmetric by definition and only the upper triangular portion is shown, and (3) the biases are only weakly coupled as desired with the highest coefficient being only 0.69 for the pair LAT2, ACT2.

The bias estimates and standard deviations calculated for the 64-superpoint set are listed in Table VII. As expected, and due primarily to the restriction on the degree of coupling permitted, the bias standard deviations are seen to be acceptably small.

The resulting value of S_ν (3.10) gives an estimate of the variances of any residual differences in the data points after application of the estimated biases. If $\sqrt{S_\nu} = 1.76$ is multiplied by the assumed range and azimuth errors (10 m and 0.5 mrad), the results 17 m and 0.88 mrad represent the residual differences between data points.

TABLE VI

COUPLING COEFFICIENTS

64 Superpoints

	AZ11	R2	AZ12	LAT2	TB12	ACT1	ACT2	ACT3
AZ11	1.0	.15	.08	.09	- .20	.01	.09	.07
R2		1.0	- .11	.59	- .16	.46	.55	.36
AZ12			1.0	- .13	- .30	.03	- .20	- .04
LAT2				1.0	- .29	.43	.69	.40
TB12					1.0	- .24	.12	- .42
ACT1						1.0	0	0
ACT2							1.0	0
ACT3								1.0

TABLE VII

BIAS ESTIMATES FROM 64-SUPERPOINT SET

	BIAS ESTIMATE	STANDARD DEVIATION
AZ11 (rad)	-0.000693	0.000126
R2 (m)	-195	9.1
AZ12 (rad)	-.2409	0.000155
LAT2 (rad)	-0.0000191	0.0000019
TB12 (msec)	-194.5	34.1
ACT1 (m)	155.5	10.8
ACT2 (m)	123.1	10.5
ACT3 (m)	249.3	11.4

ASSUMED INITIAL BIAS: AZ12 = -.2410

INITIAL S_ν = 28.1 S_ν (AFTER TWO ITERATIONS) = 3.10

Having established a set of bias estimates, the next point of interest was to investigate how well systematic error in target reports from other aircraft could be accounted for.

For the following reasons it was decided to omit the time offset bias TB12. In order to correctly process report times from the Providence sensor, the additional preprocessing described in Appendix C would have been required for each aircraft. Moreover, even if the preprocessing were performed and the time bias applied, the resulting adjustments would only be on the order of 40-50 meters and always in the direction of aircraft motion. Thus, at the plotting scales employed, the combined tracks would appear about the same whether or not a time bias was applied to the Providence reports.

Transponder delay is a bias which is different for each aircraft and not known beforehand. The approach taken here in correcting the reports from other aircraft was to use the mean value of the three transponder delays which had been calculated and are shown in Table VII.

When the corrected target reports are plotted individually for each sensor, one finds the maximum separation of tracks occurs when the aircraft is flying in the airspace between the two sensors and at a heading of 90^{o} with respect to the line connecting them. In fact, rough estimates of the transponder delay bias can be estimated using this data.

To recount the discussion above, target reports for additional aircraft were corrected for the biases designated AZ11, R2, AZ12 and LAT2 as well as a number representing an average transponder delay error. An independent set of three aircraft were used to estimate the bias values which are listed in Table VII.

Although seven additional aircraft were considered, only a few typical cases will be presented. As was true earlier, a Mercator projection is employed.

Shown in Figure 8 for aircraft code 3502 are the tracks as they are reported at Lexington and Providence before any biases are accounted for. The large

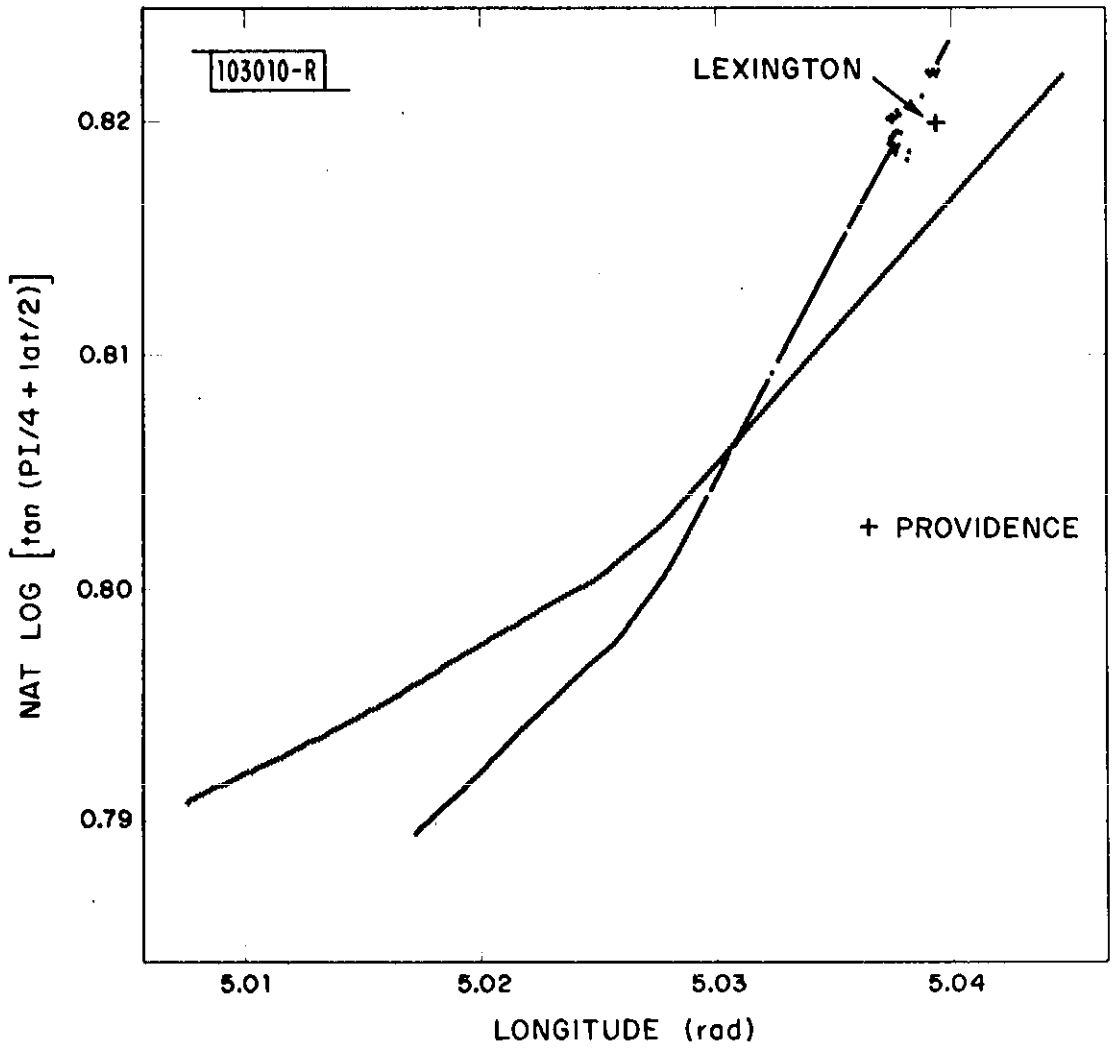

Fig. 8. Aircraft code 3502 as seen by two sensors.

azimuth offset of approximately 14^{o} in the Providence measurements is quite conspicuous. After bias removal the reports form the common track of Figure 9. The value of dual sensor coverage is demonstrated in Figure 10 where the gap and low quality of the Lexington reports is filled in quite adequately by the supporting Providence data.

Figures 11 and 12 are illustrations of the aircraft with code 2417. One interesting feature here is the apparent track segment at an azimuth of around 130^{o} from Lexington which is reported only by Lexington and not Providence. This segment was found to be a false track, i.e., a track due to reflections from an obstruction (a large semicircular antenna reflector) in the immediate vicinity of the Lexington site.

This portion of the coverage, expanded in Figure 13, also shows how the Lexington reports can be used in lieu of those from Providence just before the sharp bend in the track. The nearly one-kilometer scatter in the positions of the Providence reports is apparently due to low-elevation-angle propagation anomalies.

C. Automatic Bias Estimation

In this section two alternatives for completely automating the bias estimation are discussed. It was shown in the last section that fairly good results can be obtained by accounting for only four bias components. What is desired now is a procedure which both chooses the bias components given a set of superpoints and then solves for them. The objective is to find that combination of biases which yields a low value of S_{ν} and at the same time has consistently small coupling coefficients.

We consider two procedures. Procedure A outlined below places primary emphasis on the value of S_{ν} and secondary emphasis on the degree of coupling between the components. In Procedure B, just the reverse is true. In both it is assumed that the biases in one of the two sensors (the Lexington sensor) are small enough so that the elements of the Hessian matrix can be estimated to within a reasonable degree of accuracy. This is accomplished using simulated reports from the other sensor exactly in the manner described in the earlier section on simulation, but

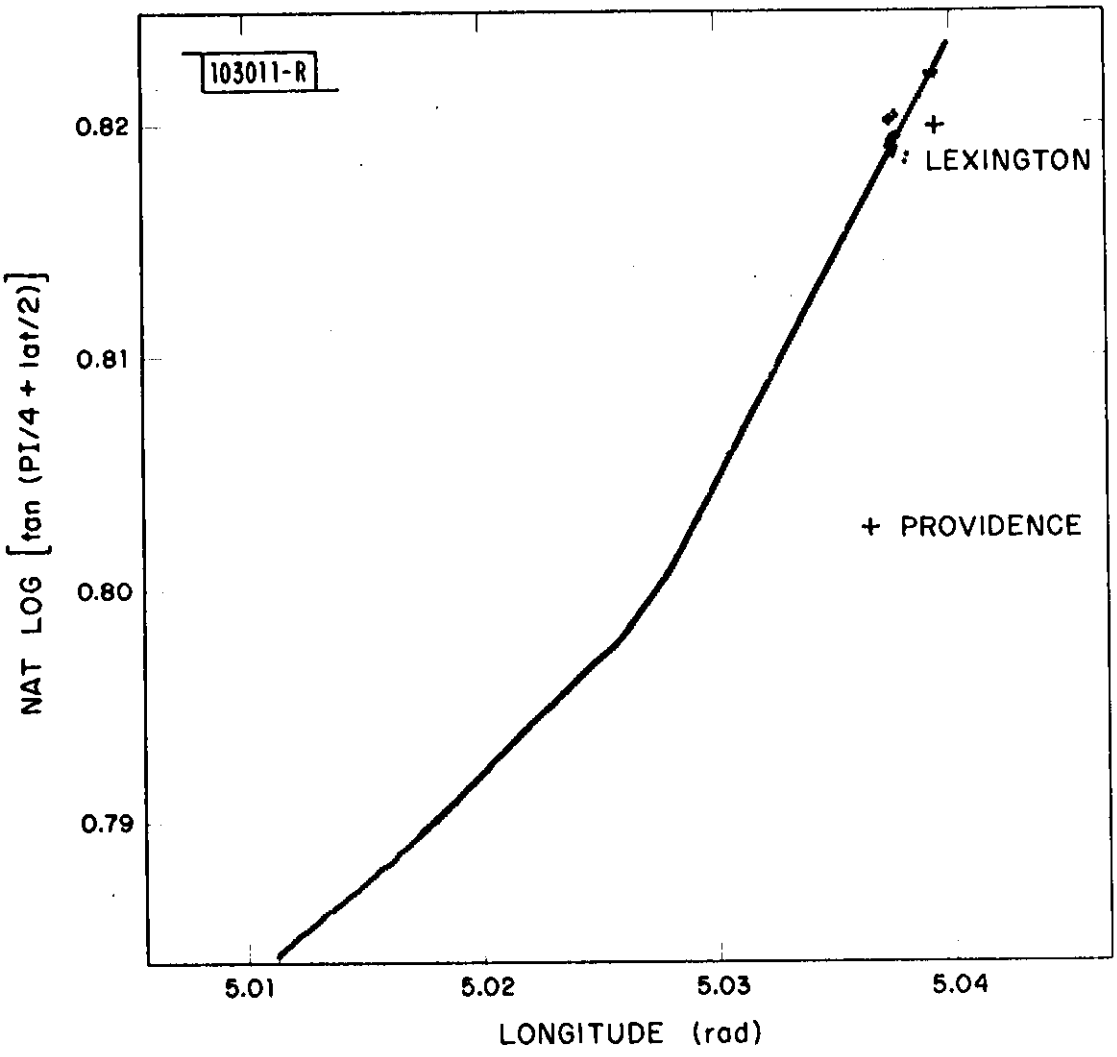

Fig. 9. Aircraft code 3502 after bias removal.

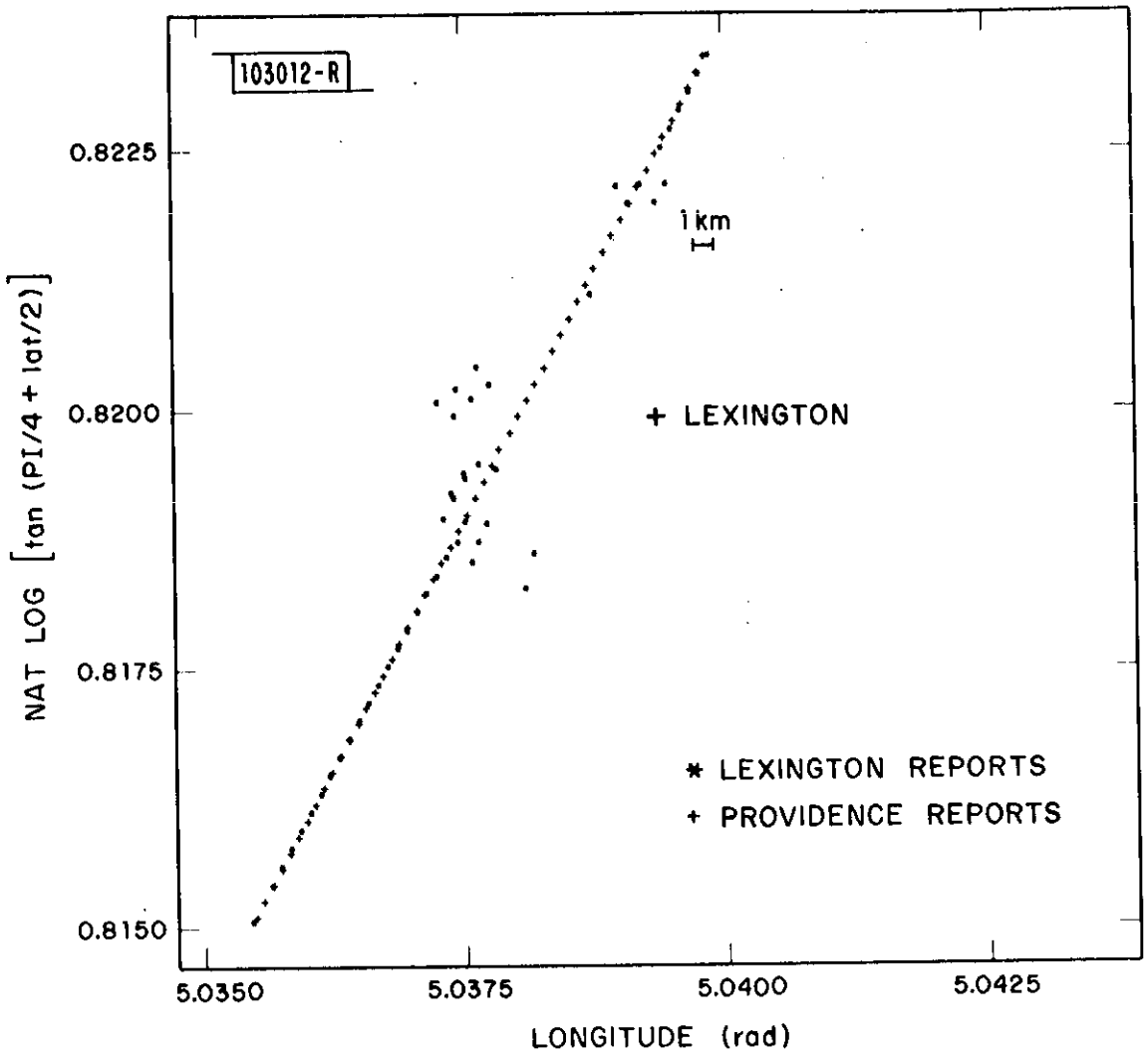

Fig. 10. Expanded view of portion of aircraft code 3502 tracks.

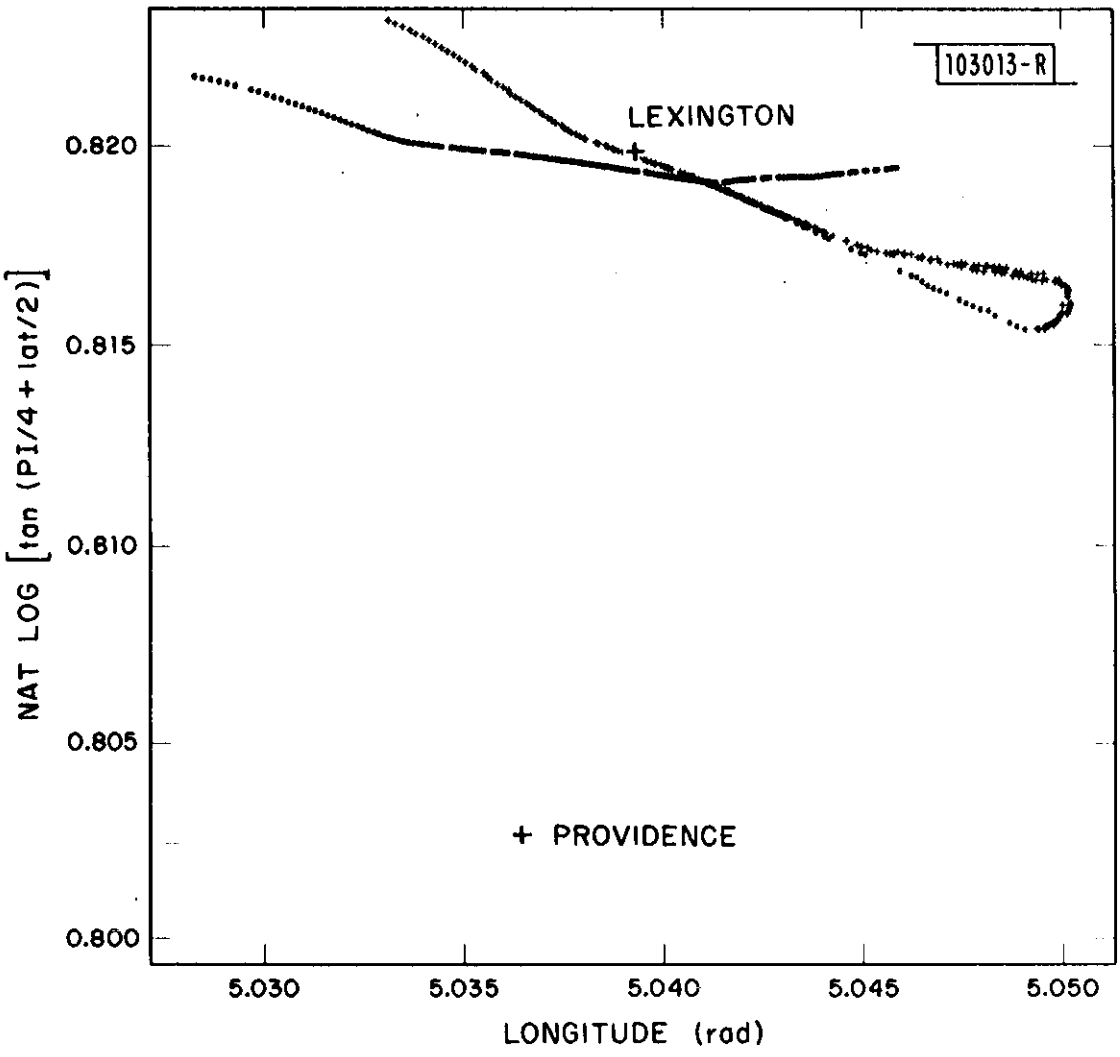

Fig. 11. Aircraft code 2417 as seen by two sensors.

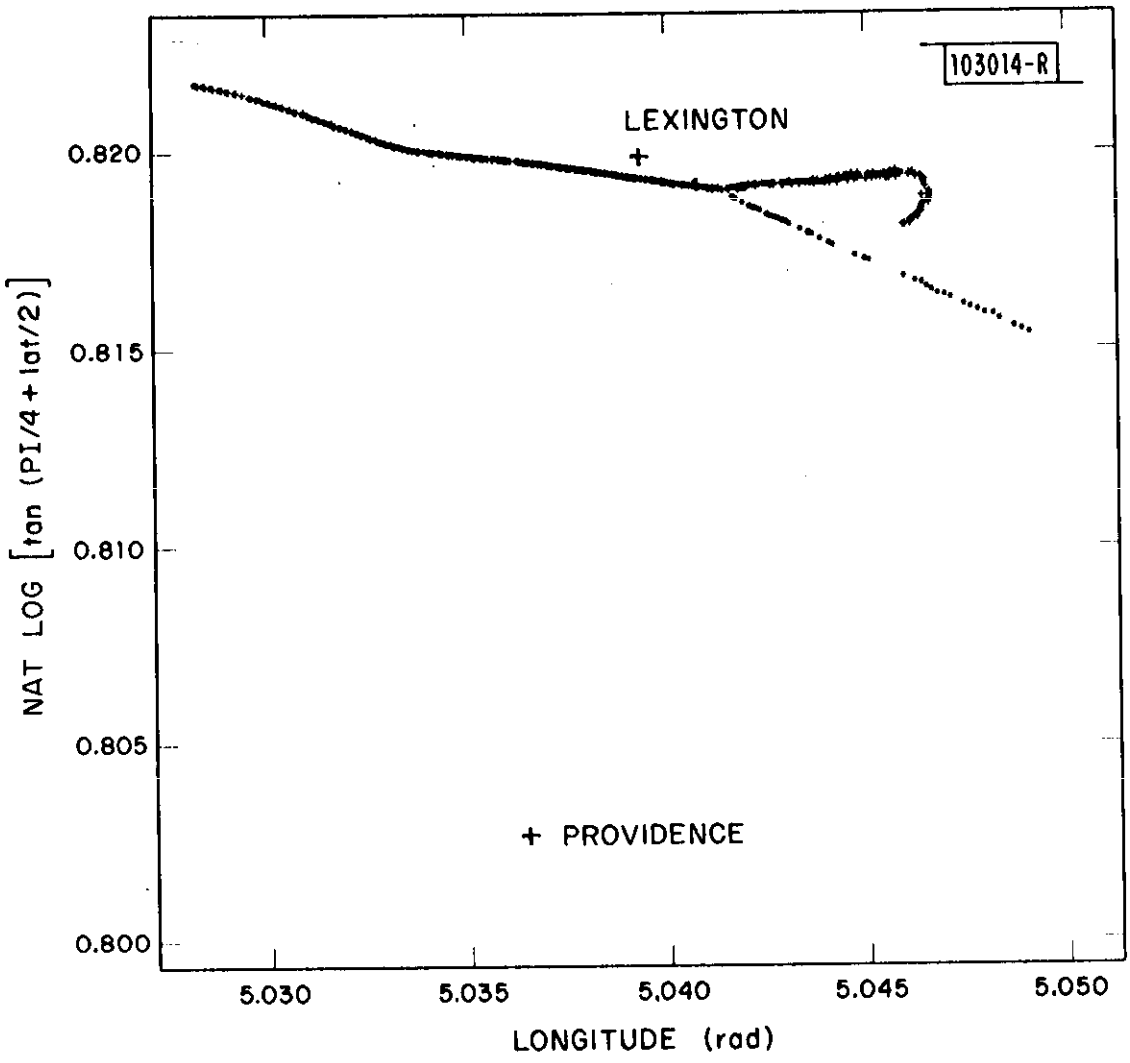

Fig. 12. Aircraft code 2417 after bias removal.

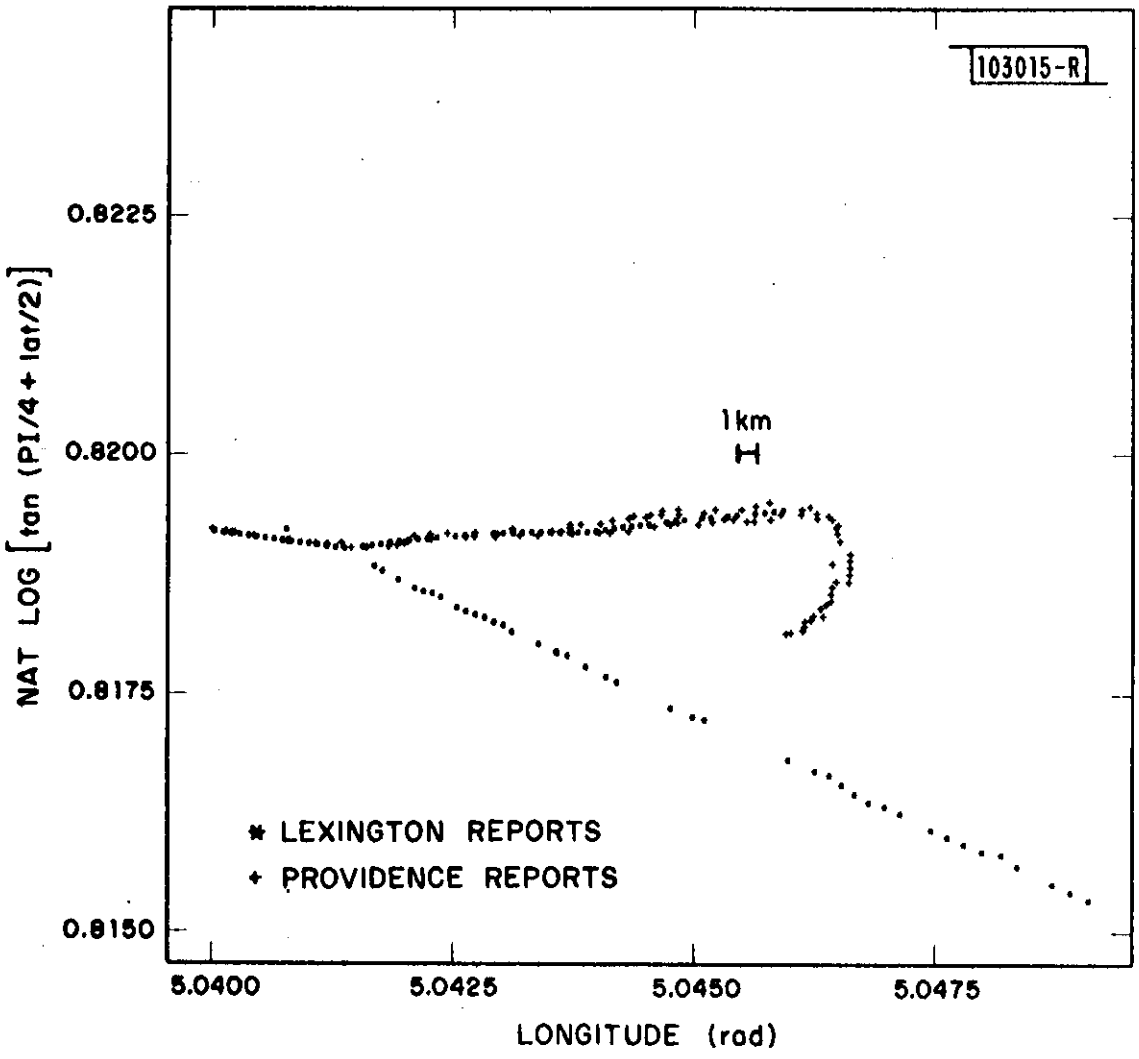

Fig. 13. Expanded view of aircraft code 2417. Observe spurious reflections from large obstruction at about 130° azimuth.

without the addition of biases. Comparisons with results obtained from real measurements have shown that this method works quite well.

Procedure A begins by computing S_ν when each of K biases is solved for individually. Recall that for one aircraft K is equal to 16.

The first bias selected is that which results in the lowest value of S_ν. This process is then repeated K-1 times with two biases (the one already selected on the previous pass and one candidate from the list of remaining components). The candidate bias, i.e., the one for which S_ν is a minimum, is added to the selected list only if the standard deviations of the already selected biases are not greater than some prescribed multiple of their standard deviation when first selected.

Thus, biases which might have a negative effect on those already selected components because of tight coupling are discarded and not considered further. Processing terminates when each of the K bias components has been either selected or discarded.

Table VIII summarizes a run of Procedure A using 23 superpoints and a multiple of 1.5 as the selection parameter. The order of entries in the table reflects the order in which the biases were selected. Thus, AZ12 was the largest bias found even when an initial value of -.2300 radian ($\sim$-13.2 deg) was assumed for it.

One variation on this method would be to use the degree of coupling between the candidate bias and the previously selected biases as an accept/reject criterion. This would reduce the amount of computation since the full Hessian matrix is computed only once at the beginning of the run and the matrix inversion performed in computing the bias standard deviation could be avoided.

Procedure B places greater emphasis on the degree of coupling between the bias components and then utilizes the calculated S_ν values as a final selector.

As was the case in Procedure A, the elements of the Hessian matrix are calculated and from them the coupling coefficients between the K bias components.

TABLE VIII

AUTOMATIC BIAS SELECTION AND ESTIMATION

PROCEDURE A

23 Superpoints

Aircraft Code = 4655

Assumed Biases: AZ12 = -.2300

Multiplier = 1.5

Final Value of S_ν = 4.01

COMPONENT	ESTIMATED VALUE	STANDARD DEVIATION
AZ12	- .2405	0.00053
AZ31	-0.0089	0.00267
RC1	0.0019	0.000301
TB22	-0.000138	0.000045
LON2	-0.000013	0.000006
R2	-35.74	17.99
AZ32	0.00460	0.0046
AZ41	-0.0014	0.0030
AZ42	-0.00081	0.0039

Then, establishing a cut-off on the magnitude of the coupling permitted, N combinations of J biases each are formed. These N combinations each constitute a weakly coupled set such that no set with greater than J biases could be created.

For each of the N combinations S_ν is calculated, and the final choice is based on which results in minimum S_ν. In cases where several combinations yield values of S_ν, all within the calculated standard deviation of S_ν, approximately $2/\nu$, then the combination with the uniformly lowest coupling would be selected.

The 64-superpoint data set described earlier and shown in Figure 4 was the basis for testing Procedure B. When a limit of 0.5 was placed on the largest coupling coefficient it was found that 54 combinations of eight biases each could be formed. There were none with nine or more combinations. Table IX lists values calculated for the combination which resulted in minimum S_ν.

Both procedures have attributes which are not satisfactory.

1. They require selection parameters which can affect the final outcome.
2. They are dependent on initial, assumed bias estimates.
3. They consume a great deal of computer processing time.

Of the two approaches Procedure B seems to be preferable. It is faster and relies less on assumptions concerning initial bias values. Moreover, intuition seems to favor the generation of conservative estimates of only a few biases at the expense of having to accept larger residual errors. Then as more data becomes available in additional coverage areas, new bias estimates can be optimally combined with previous estimates in the manner suggested in Appendix D.

VII. CONCLUSIONS

The problem of accurately registering sensors in a network has been studied. There are many possible sources of calibration errors affecting the registration accuracy. These include such things as azimuth, range and time offset biases, errors in sensor location, etc. When all of these error sources are eliminated, and when accurate coordinate conversion equations are employed, various sensor

TABLE IX

AUTOMATIC BIAS SELECTION AND ESTIMATION

PROCEDURE B

64 Superpoints

Assumed Bias: AZ12 = -.2400

Coupling Coefficient Limit = 0.5

S_ν = 3.16

COMPONENT	ESTIMATED VALUE	STANDARD DEVIATION
AZ11 (rad)	-0.00054	0.00013
RC1	0.00019	0.000057
RC2 (m)	-88.7	6.2
AZ31 (rad)	-0.0129	0.00135
AZ22 (rad)	-0.0049	0.00085
TB22	-0.00011	0.0000256
ACT1 (m)	57.7	6.15
ACT3 (m)	148.1	6.97

outputs will register with the accuracies determined by measurement accuracies of the individual sensors.

A self-registration algorithm was developed to check for bias errors and to find a set of bias corrections which will cause good registration over the whole common coverage of two sensors. Usually all of the possible biases cannot be determined unambiguously due to the coupling effect between biases. This coupling effect and its impact on the variance of the bias estimates are also evaluated by the self-registration algorithm and can be used as criteria for the choice of a subset of all possible biases so as to provide adequate registration accuracy.

The self-registration algorithm was tested by analyzing both simulated and real data from two sensors spaced about 45 nmi apart. The results demonstrated the essential accuracy of the algorithm and provided final rms registration accuracies of about one milliradian in azimuth and 20 meters in range which is about twice the measurement accuracies of the individual sensors. Indeed the registration was good enough to easily discern areas of increased sensor error. This increased error was generally confined to low-elevation aircraft and could usually be traced to obstructions near the sensor.

The self-registration algorithm developed in this study is not considered a cure-all for registration problems. The factors limiting registration accuracy should be corrected at their source. Tilt meters, north-seeking gyros and external sensor position-location systems should be employed. Accurate clocks and a system for clock registration should be used. Range offsets and antenna tilt should be carefully calibrated. Because of the coupling among the biases described above, the self-registration algorithm should only be used as an overall check of registration accuracy to discover items not properly calibrated or to refine a few biases.

The ability to accurately register the output of sensors with overlapping coverage now allows the development of multi-sensor trackers. A multi-sensor tracker accepts target reports from more than one sensor and forms a single track for each aircraft. Multi-sensor tracking provides the advantages enumerated in the Introduction; namely, improved track quality, identity maintenance, large area coverage including low flyers and resistance to enemy countermeasures. In addition,

a multi-sensor network provides the basis for inclusion of other types of information such as radio direction finder reports and aircraft position reports derived from on-board aircraft navigation systems.

The registration accuracy demonstrated in this study is considerably better than that customarily achieved. In order to take full advantage of this increased accuracy the transmission of more significant bits in the reporting message formats will be required. The formats should also include target report time tags. Lastly, it is recommended that all reports be in geodetic coordinates to allow easy correlation with other data already in geodetic coordinates and to allow an integrated system of sensors to grow naturally over an extended area.

ACKNOWLEDGMENTS

We would like to take this opportunity to acknowledge the help of the following Lincoln Laboratory personnel. Jack Mitchell provided several useful discussions and analyses regarding the coordinate conversion problem. A. Kaminsky provided the data tapes and instructed us in their use. Gary Duff examined the data to confirm some anomalies. Discussions with Joe Salah helped resolve some sensor calibration questions, and Linda Wesley prepared the manuscript.

We would also like to thank our sponsors, Joe Allen of CORADCOM and Tom Maggio and Len Strauss of RADC for their support and encouragement.

REFERENCES

1. "National Airspace System Configuration Management Document, Multiple Radar Data Processing," Report No. NAS-MD-320, Federal Aviation Administration, Department of Transportation (15 May 1973).

2. D. Goldenberg and E. W. Wolf, "A Common Coordinate System for the Utilization of Data from Several Radars," Technical Report 67, Lincoln Laboratory, M.I.T. (13 September 1954), DDC AD-50611.

3. E. Wolf, "A Stereographic Coordinate System for the Utilization of Data from Several Radars," Report SR-2, The MITRE Corporation (March 1959).

4. R. G. Mulholland, D. W. Stout, "Numerical Studies of Conversion and Transformation in a Surveillance System Employing a Multitude of Radars, Part I," Report No. FAA-NA-79-17, Part II, Report No. FAA-NA-79-18, National Aviation Facilities Experimental Center, Federal Aviation Administration, Department of Transportation (April 1979).

5. M.J.D. Powell, Comp. J. 7, 155-162 (1964).

6. R. P. Brent, Algorithms for Minimization without Derivatives (Prentice-Hall, Englewood Cliffs, New Jersey, 1973).

7. W. L. Oliver, "Millstone Hill Radio Star Calibration Observations," Project Report STK-103, Lincoln Laboratory, M.I.T. (9 August 1979), DDC AD-A079037/8.

8. KREMS Metric Calibration Manual, Lincoln Manual 121, Lincoln Laboratory, M.I.T. (15 September 1977), not generally available.

9. Formulae and Tables for Computation of Geodetic Positions, U.S. Coast and Geodetic Survey, Special Publication No. 8 (1919).

10. G. E. Forsythe, J. Soc. Indus. Appl. Math. 5, 74-88 (1957).

11. J. L. Gertz, "The ATCRBS Mode of DABS," Project Report ATC-65, Lincoln Laboratory, M.I.T. (31 January 1977).

12. D. A. Spencer, "DABSEF SDP Data Recording Formats," private communication.

13. J. Pellegrino, "TMF Data Reduction," private communication.

APPENDIX A

PROPAGATION DELAY IN ATMOSPHERE

The correction to range for the effect of atmospheric refraction is based on the following steps:

1. Calculate target elevation angle η from the expression:

$$\eta = \sin^{-1} \left(\frac{H^2 - H_r^2 + 2E(H - H_r) - R^2}{2R(E + H_r)} \right)$$

where:

H = target altitude

H_r = radar altitude

R = target range

E = mean earth radius

2. With range and elevation, refer to Table A-1 for the correction value.

   a. Use logarithmic interpolation for ranges and elevations not found directly as entries into the Table.

TABLE A-1

RANGE REFRACTION CORRECTION (ref. 8)
(meters)

Range (km) \ Elevation (deg)	0.01	1.00	2.00	3.00	4.00	5.00	6.00	7.00	8.00	9.00
0.01	0.004	0.004	0.004	0.004	0.004	0.004	0.004	0.004	0.004	0.004
5.00	1.866	1.853	1.840	1.828	1.815	1.803	1.791	1.779	1.767	1.755
10.00	3.731	3.680	3.630	3.580	3.532	3.485	3.438	3.393	3.348	3.304
15.00	5.594	5.481	5.369	5.261	5.155	5.053	4.953	4.857	4.763	4.672
20.00	7.455	7.255	7.059	6.871	6.690	6.515	6.347	6.185	6.029	5.878
25.00	9.314	9.002	8.701	8.414	8.139	7.877	7.627	7.388	7.160	6.942
30.00	11.169	10.722	10.295	9.891	9.508	9.146	8.803	8.479	8.172	7.886
35.00	13.021	12.416	11.842	11.305	10.801	10.328	9.884	9.467	9.087	8.738
40.00	14.867	14.082	13.344	12.658	12.020	11.427	10.875	10.375	9.922	9.507
50.00	18.545	17.331	16.212	15.190	14.256	13.405	12.654	11.984	11.379	10.826
60.00	22.198	20.470	18.905	17.502	16.243	15.151	14.199	13.351	12.589	11.898
70.00	25.820	23.497	21.431	19.610	18.035	16.701	15.539	14.511	13.595	12.780
80.00	29.408	26.413	23.796	21.535	19.659	18.073	16.699	15.496	14.442	13.509
90.00	32.958	29.216	26.005	23.314	21.127	19.286	17.704	16.342	15.155	14.110
100.00	36.463	31.906	28.066	24.957	22.452	20.356	18.582	17.067	15.754	14.594
150.00	53.198	43.697	36.620	31.402	27.366	24.161	21.506	19.224	17.289	15.655
200.00	68.279	52.976	42.776	35.610	30.279	26.004	22.586	19.858	17.663	15.877
400.00	108.510	72.528	52.598	40.432	32.506	27.036	23.076	20.097	17.782	15.938
800.00	126.910	76.609	53.607	40.737	32.618	27.086	23.102	20.112	17.792	15.945
4000.00	132.590	77.815	53.986	40.890	32.692	27.128	23.129	20.131	17.807	15.958

Range (km) \ Elevation (deg)	10.00	12.00	14.00	17.00	20.00	25.00	30.00	40.00	60.00	89.99
0.01	0.004	0.004	0.004	0.004	0.004	0.004	0.004	0.004	0.004	0.004
5.00	1.743	1.720	1.698	1.665	1.634	1.585	1.540	1.462	1.350	1.290
10.00	3.261	3.178	3.098	2.985	2.879	2.719	2.580	2.358	2.074	1.930
15.00	4.583	4.413	4.254	4.032	3.836	3.556	3.320	2.950	2.498	2.280
20.00	5.733	5.460	5.212	4.885	4.600	4.194	3.858	3.351	2.747	2.452
25.00	6.735	6.360	6.028	5.592	5.212	4.683	4.258	3.625	2.865	2.521
30.00	7.623	7.147	6.727	6.177	5.706	5.065	4.557	3.787	2.920	2.549
35.00	8.416	7.835	7.324	6.663	6.109	5.363	4.764	3.877	2.944	2.561
40.00	9.123	8.436	7.835	7.072	6.440	5.585	4.896	3.928	2.956	2.566
50.00	10.318	9.421	8.659	7.708	6.913	5.838	5.033	3.972	2.963	2.568
60.00	11.274	10.190	9.279	8.127	7.171	5.955	5.088	3.985	2.965	2.569
70.00	12.049	10.789	9.718	8.372	7.309	6.009	5.110	3.990	2.965	2.569
80.00	12.677	11.232	9.999	8.515	7.382	6.034	5.119	3.991	2.965	2.569
90.00	13.176	11.531	10.177	8.597	7.421	6.046	5.123	3.991	2.965	2.569
100.00	13.538	11.733	10.290	8.645	7.442	6.051	5.124	3.992	2.966	2.569
150.00	14.273	12.088	10.465	8.707	7.464	6.056	5.125	3.992	2.966	2.569
200.00	14.405	12.136	10.482	8.711	7.466	6.056	5.126	3.992	2.966	2.569
400.00	14.437	12.147	10.487	8.713	7.467	6.057	5.126	3.993	2.966	2.570
800.00	14.442	12.150	10.489	8.715	7.468	6.058	5.127	3.994	2.968	2.571
4000.00	14.453	12.159	10.498	8.723	7.476	6.065	5.134	4.000	2.973	2.576

APPENDIX B

COORDINATE TRANSFORMATIONS

A. *Cartesian Coordinates Given Geodetic Coordinates*

We first derive equations for converting between geodetic coordinates latitude ϕ, longitude λ, and altitude H, above mean sea level and x, y, z coordinates whose center is at the earth's center. As shown in Figure B-1, the z axis coincides with the earth's axis of rotation and the x axis passes through the Greenwich meridian. The earth has a radius "a" at the equator and "b" at the poles. Latitude is defined as the angle ϕ that a normal at the earth's surface makes with its projection on the equatorial plane. The eccentricity "e" is defined as:

$$e^2 = \frac{a^2 - b^2}{a^2} \tag{B1}$$

From the properties of an ellipse (see Figure B-2) it can be shown that the normal nℓ terminating at the major axis equals:

$$\frac{b^2}{a\ (1 - e^2\ \sin^2\ \phi)^{1/2}} \tag{B2}$$

The normal nm produced to the minor axis equals:

$$N = \frac{a}{(1 - e^2\ \sin^2\ \phi)^{1/2}} \tag{B3}$$

Using these values and referring to Figure B2, it is easily seen that the following equations convert geodetic coordinates to x, y, z coordinates.

$$z = \left[\frac{a\ (1 - e^2)}{(1 - e^2\ \sin^2\ \phi)^{1/2}} + H\right] \sin\ \phi \tag{B4}$$

Letting line segment cd be called s in Figure B-2,

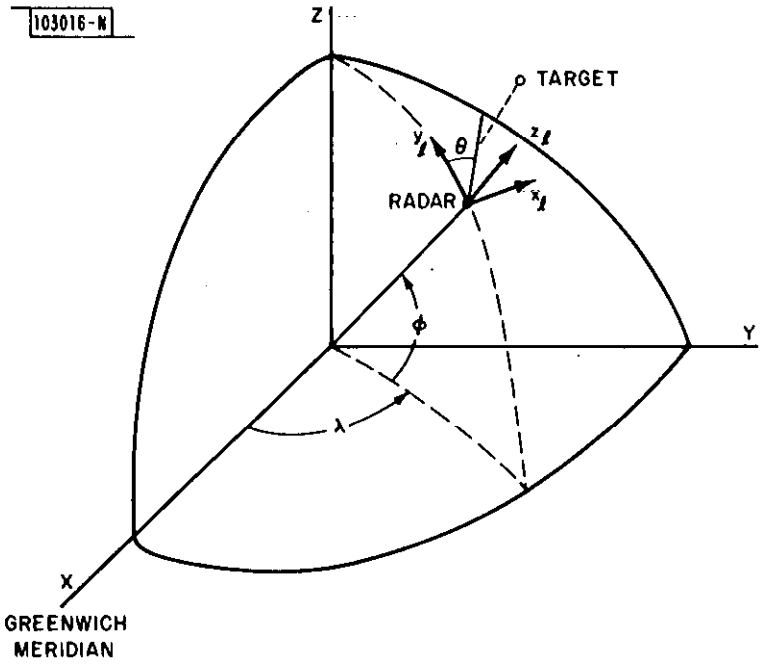

Fig. B-1. Coordinate geometrics.

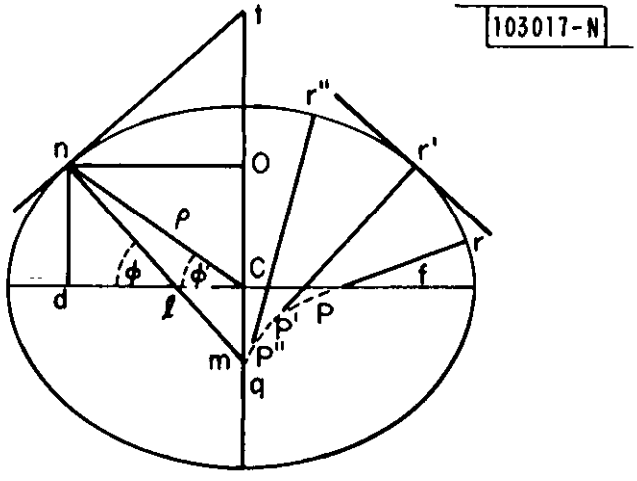

Fig. B-2. Cross section of Earth through its axis

$$s = \left[\frac{a}{(1 - e^2 \sin^2 \phi)^{1/2}} + H \right] \cos \phi \qquad \text{(B5)}$$

$$x = s \cos \lambda \qquad \text{(B6)}$$

$$y = s \sin \lambda \qquad \text{(B7)}$$

B. Radar Coordinates to Geodetic Coordinates

Accurate conversion from radar coordinates to geodetic coordinates can be accomplished in three steps. The radar coordinates (range, azimuth, and elevation) are first converted into local Cartesian coordinates. The local coordinates are then rotated and translated into earth-centered Cartesian coordinates. Finally, the earth-centered coordinates are converted to geodetic coordinates (latitude, longitude, and altitude above mean sea level). We will describe each of these steps in turn.

(1) The local Cartesian coordinates are:

$$x_\ell = R \cos \eta \sin \theta \qquad \text{(B8)}$$

$$y_\ell = R \cos \eta \cos \theta \qquad \text{(B9)}$$

$$z_\ell = R \sin \eta \qquad \text{(B10)}$$

where

z_ℓ points toward the zenith,

y_ℓ points toward the north,

x_ℓ points toward the east,

θ is the azimuth measured clockwise from north,

R is the slant range, and

η is the elevation angle to the target.

It is assumed that R and η have been corrected for propagation effects in the earth's atmosphere.

(2) The local coordinates are next transformed into earth-centered coordinates.

$$\begin{bmatrix} x \\ y \\ z \end{bmatrix} = T_R \begin{bmatrix} x_\ell \\ y_\ell \\ z_\ell \end{bmatrix} + \begin{bmatrix} x_r \\ y_r \\ z_r \end{bmatrix} \tag{B11}$$

where T_R is the rotation matrix which rotates the local coordinate system to align it with the earth-centered coordinate system.

$$T_R = \begin{bmatrix} -\sin \lambda_r & -\cos \lambda_r \sin \phi_r & \cos \lambda_r \cos \phi_r \\ \cos \lambda_r & -\sin \lambda_r \sin \phi_r & \sin \lambda_r \cos \phi_r \\ 0 & \cos \phi_r & \sin \phi_r \end{bmatrix} \tag{B12}$$

The second vector in the above equation is the location of the center of the radar in earth-centered coordinates. This is determined using Eqs. (B4) through (B7) and using ϕ, λ, and H equal to the coordinates of the radar.

(3) Finally, we convert the earth-centered Cartesian coordinates to geodetic coordinates. To solve for the latitude ϕ and altitude H, it would be logical to invert equations (B4) and (B5), but this would necessitate the solution of a higher order equation. Instead, we first solve for H using the original data and then use H in equations (B4) and (B5) to solve for ϕ.

Using the construction of Figure B-3 and the law of cosines, we find

$$H = [(E + H_r)^2 + R^2 + 2R (E + H_r) \sin \eta)]^{1/2} - E \tag{B13}$$

where: H_r is the radar's altitude and E is the mean earth radius, (a + b)/2. Using the mean earth radius instead of solving exactly in spheroidal coordinates introduces a maximum error of 25 m in H at a range of 300 km increasing as R^2. This is a negligible height error and, in addition, causes a still smaller error in determining latitude ϕ.

Next in determining ϕ, the square root term is eliminated between (B4) and (B5), yielding:

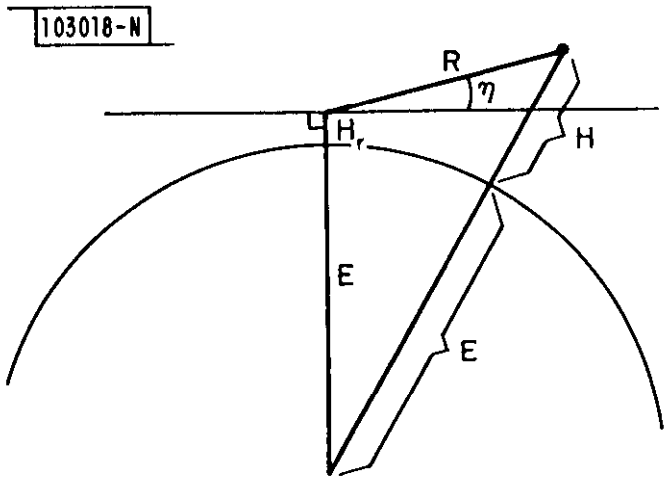

Fig. B-3. Construction for estimating aircraft height.

$$\tan \phi = \frac{z}{\rho \ (1 - e^2) + e^2 \ H \cos\phi} \tag{B14}$$

where: $\rho = (x^2 + y^2)^{1/2}$.

This can be evaluated in two steps. A first estimate of ϕ is made:

$$\tan \phi_1 = \frac{z}{\rho \ (1 - e^2)} \tag{B15}$$

Then the final value is determined

$$\tan \phi = \frac{z}{\rho \ (1 - e^2) + e^2 \ H \cos \phi_1} \tag{B16}$$

The size of the second term in the denominator of (B14) is about 1/3000 of the first term for a high-altitude aircraft. Thus, the approximation of Eq. (B16) is correct to about one part in 10^7, which is an entirely negligible error.

Finally, the longitude is determined:

$$\tan \lambda = \frac{y}{x} \tag{B17}$$

The above conversion process might seem rather lengthy. It actually involves the determination of only six trigonometric functions, 24 multiplies or divides and two square roots.

C. Beacon Coordinates to Geodetic Coordinates

A beacon transponder system produces height instead of elevation angle. Using Eq. (B13),

$$z_\ell = R \sin \eta = \frac{H^2 - H_r^2 + 2 \ (H - H_r) \ E - R^2}{2 \ (E + H_r)} \tag{B18}$$

$$x_\ell = R \sqrt{1 - (\frac{z_\ell}{R})^2} \ \sin \theta \tag{B19}$$

$$y_\ell = R \sqrt{1 - (\frac{z_\ell}{R})^2} \ \cos \theta \tag{B20}$$

Equations (B11) to (B17) are then used to find the earth coordinates.

D. Geodetic Coordinates to Local Coordinates

It will often be required to transform from geodetic coordinates (latitude, longitude, and altitude) to local coordinates. For instance, local coordinates (azimuth, elevation, and range) are required to aim an air defense missile against a target.

(1) Geodetic coordinates (ϕ, λ, H) are first converted to earth-centered (z, y, z) using Eqs. (B4) through (B7).

(2) Local coordinates (x_ℓ, y_ℓ, z_ℓ) are generated using:

$$\begin{bmatrix} x_\ell \\ y_\ell \\ z_\ell \end{bmatrix} = T_R^T \begin{bmatrix} x \\ y \\ z \end{bmatrix} - T_R^T \begin{bmatrix} x_r \\ y_r \\ z_r \end{bmatrix} \tag{B21}$$

where: x_r, y_r, z_r are the coordinates of the air defense weapon and T_R^T is the transpose of the rotation matrix in Eq. (B12).

Finally, R, θ and η are determined.

$$R = (x_\ell^2 + y_\ell^2 + z_\ell^2)^{1/2} \tag{B22}$$

$$\tan\theta = \frac{x_\ell}{y_\ell} \tag{B23}$$

$$\tan\eta = \frac{z_\ell}{\sqrt{x_\ell^2 + y_\ell^2}} \tag{B24}$$

E. Reference Ellipsoids

The earth model employed in this investigation is the DoD World Geodetic System 1972 reference ellipsoid. Another model, often used in local surveying, is called the Clarke 1866 ellipsoid. The important parameters of both models

are given in Table B-1. Bias estimation test runs indicated little sensitivity to choice of model at the latitudes and longitudes considered here.

TABLE B-1

REFERENCE ELLIPSOIDS

MODEL	SEMI-AXES MAJOR A	MINOR B	FLATTENING FACTOR
DoD WGS-72	6378135 m	6356751 m	1/298.26
Clarke 1866	6378206 m	6356585 m	1/295.0

F. Single Precision Coordinate Transformation

The exact coordinate transformations described above require double precision arithmetic.

A very accurate, single precision coordinate transformation from sensor coordinates to geodetic coordinates is obtained by expansion of the earth-surface arc length in series form (ref. 9). In what follows R, H, and θ are the target range and height above sea level and azimuth. H_r, ϕ_r, and λ_r are the radar height above sea level and latitude and longitude, and a and e^2 are the earth's radius at the equator and eccentricity squared. For sensor ranges less than 350 km the central angle represented by the arc length σ is given to one-meter accuracy by:

$$\sigma = 2 \arcsin(\sigma_o/2) \simeq \sigma_o + \frac{\sigma_o^3}{24} \tag{B25}$$

where:

$$\sigma_o = \sqrt{\frac{R^2 - (H - H_r)^2}{(\rho_1 + H)\quad(\rho_1 + H_r)}} \tag{B26}$$

and

$$\rho_1 = \frac{a\,(1 - e^2)}{(1 - e^2 \sin^2 \phi_r)^{3/2}} \tag{B27}$$

The target's latitude is given by first calculating:

$$\delta\phi = \sigma \cos\theta - \left[\frac{\tan\phi_r}{2} \cdot \frac{\rho_1}{\rho_2}\right] \sigma^2 \sin^2\theta$$

$$- \left[\frac{(1 + 3\tan^2\phi_r}{6} \left(\frac{\rho_1}{\rho_2}\right)^2\right] \sigma^3 \sin^2\theta \cos\theta$$

$$1\ [1 + 3\tan^2\phi_r - (9 + 15\tan^2\phi_r)\cos^2\theta] \left(\frac{\rho_1}{\rho_2}\right)^3 \tan\phi_r\ \sigma^4 \sin^2\theta \quad \text{(B28)}$$

then:

$$\phi = \phi_r + \delta\phi - (\delta\phi)^2 \left[\frac{3\, e^2 \sin\phi_r \cos\phi_r}{2\,(1 - e^2 \sin^2\phi_r)^{3/2}}\right] \quad \text{(B29)}$$

The above equation for target latitude was derived using the law of cosines for spherical triangles which gives cos σ and expanding in a series about the sensor latitude. Using the law of sines for spherical triangles, we find:

$$\lambda = \lambda_r + \arcsin\left(\frac{\sin\theta \sin\sigma_1}{\cos\phi}\right)$$

$$= \lambda_r + \frac{\sigma_1 \sin\theta}{\cos\phi} - \frac{\sigma_1^3 \sin\theta}{6\cos\phi} + \frac{\sigma_1^3 \sin^3\theta}{6\cos^3\phi} \quad \text{(B30)}$$

where:

$$\sigma_1 = \frac{\sigma\rho_1 (1 - e^2 \sin^2\phi)^{1/2}}{a} \quad \text{(B31)}$$

The above equations were checked for accuracy by calculating latitudes and longitudes at many azimuth angles for sensor ranges out to 350 km. The results were compared with those calculated using the very accurate equations presented in the first part of this Appendix. The maximum differences are presented in Figs. B-4 and B-5. We see in Fig. B-4 that adequate accuracies are achieved up to about 45 degrees latitude using a four-term expansion. This accuracy can be extended to 70° by using a fifth term (the fourth term in Eq. B28). These curves are independent of target height to well above 18 km.

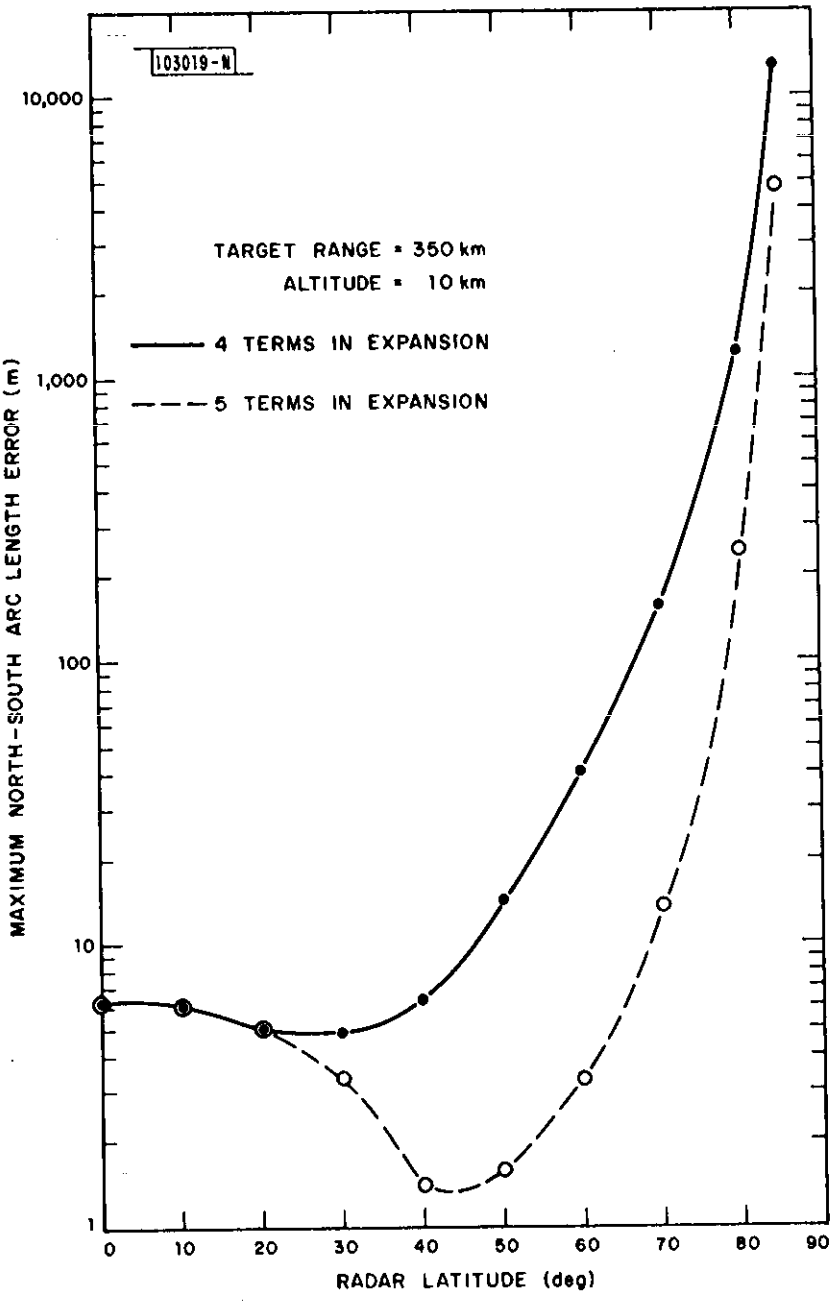

Fig. B-4. Maximum errors introduced by using series approximations for target latitude.

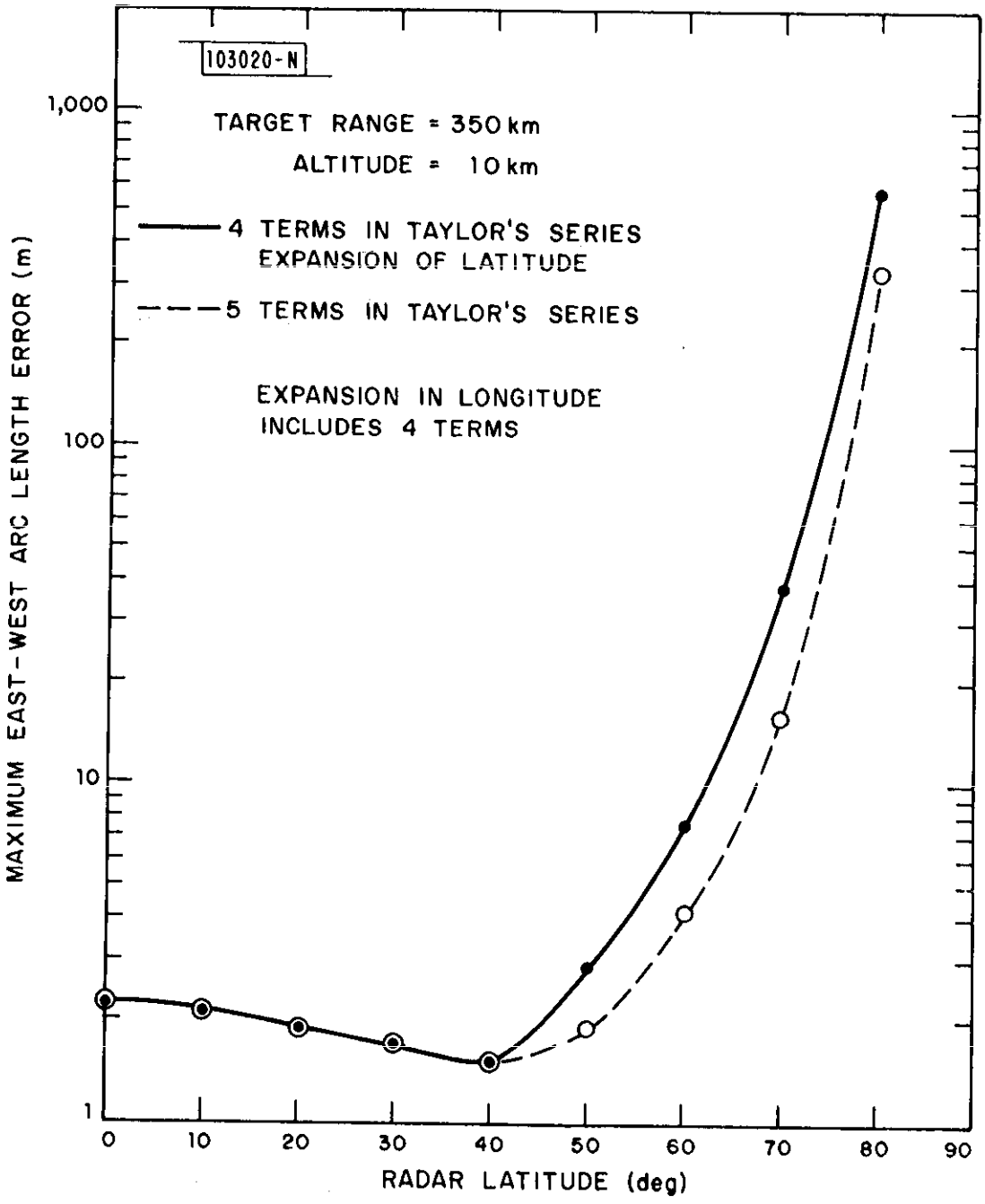

Fig. B-5. Maximum errors introduced by using series approximations for target longitude.

APPENDIX C
DESCRIPTION OF PRE-PROCESSING

A. Introduction

Data employed in this study were recorded simultaneously at each of two Air Traffic Control Radar Beacon System (ATCRBS) sites, Lexington, Mass. and Providence, R.I.

The target reports which comprise the basic data have already been preprocessed by reply correlation and centroiding into target reports as well as target-to-track association. An extensive documentation of that surveillance processing software is available in ref. 11 and it should be consulted for additional detail.

In this study, two data sources have been used to create a test data base. The first consists of observations of range, azimuth, altitude, and aircraft identification code and is called the System Demonstration Program (SDP) tape (ref. 12). The other source is derived from the SDP tape and is valuable for editing and for the time-base correction which is described below. This latter tape is referred to as a ZFLAG tape because of the presence of flag words which are used to qualify each target report (ref. 13).

In the remaining sections of this Appendix, a brief description of each of the main data preparation steps performed on the SDP data will be given. These steps are summarized graphically in Figure C-1.

B. Determination of Accurate Target Report Times

The time associated with a target report is the time at which the block itself was recorded by the ATCRBS target-to-track correlation task and, therefore, not necessarily the desired observation time.

In order to rectify this situation and generate a more accurate target tag time required by this study, a procedure was developed based on matching the "average" azimuth value associated with a target report on the ZFLAG tape with azimuths of individual replies on the SDP tape. Once this match is achieved, the new, more accurate time is obtained by linear interpolation.

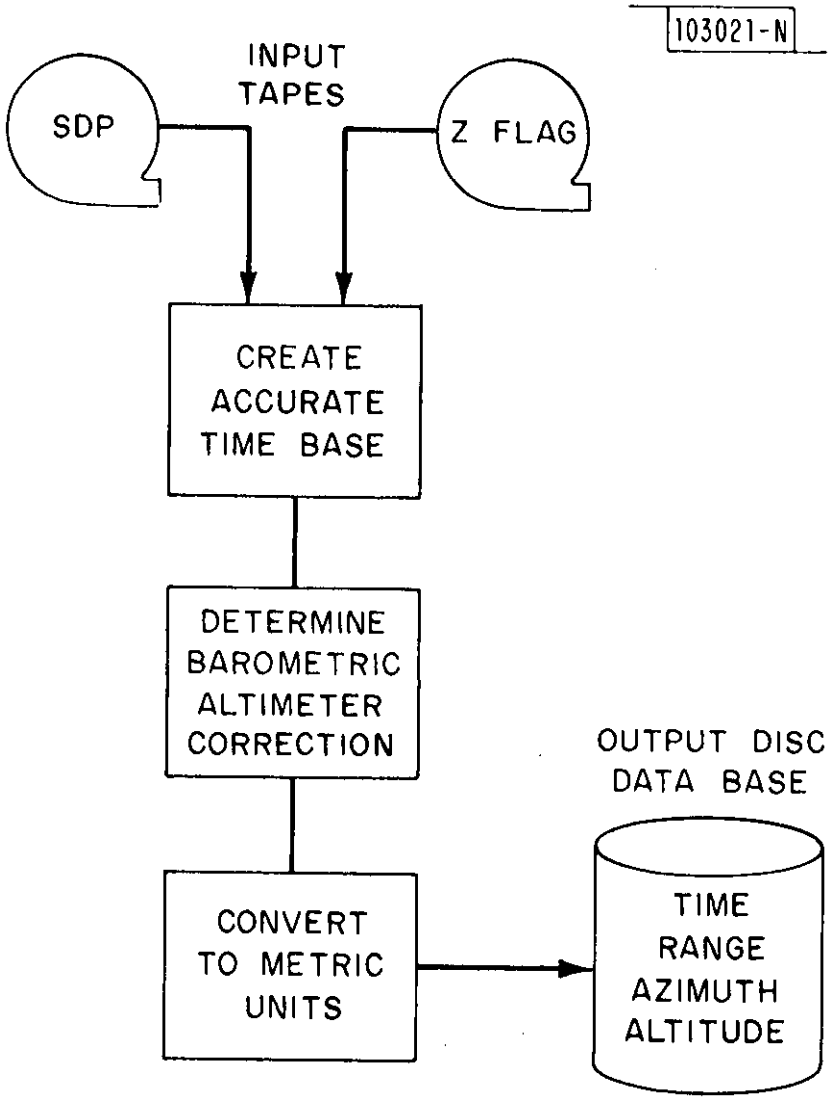

Fig. C-1. Main steps in data preparation.

Since the time between reply blocks is 10 ms, the calculated report time is accurate to within a few milliseconds and is entirely adequate for the estimation of a time bias between the two sensors.

Shown in Figure C-2 is a time interval during which the aircraft having a code of 4655 was executing a steep ascent maneuver. After the time has been accurately determined for both sensors, a time offset of approximately 1500 ms can be readily discerned. This relative time offset was found in the data from other aircraft and was used as the initial best estimate of the time bias TB12.

C. Altitude Correction

The altitude recorded on both the Lexington, Mass., and Providence, R.I., data tapes is not corrected for barometric pressure. Fortunately, simultaneous SDP data tapes were also available from the ARTS-III sensor at Logan International Airport in Boston, Mass.

In the ARTS system the altitude recorded in the target report block reflects an altitude correction not made to the altitude appearing in the reply block. Thus, the difference between the report block altitude and the reply block altitude for an ARTS target is the adjustment which is to be applied to the target report at Lexington and Providence.

It was found that an altitude correction of 300 ft had to be added to both the Lexington and Providence data.

D. Conversion to Metric Units

In this final phase of data preparation, the target report records are converted from units used on the SDP tape (ref. 12) to range and altitude in meters and azimuth in radians. Due consideration is given to the range clock settings at each sensor.

Some data editing is also performed. For example, target reports with questionable altitude values are not copied into the final test data base.

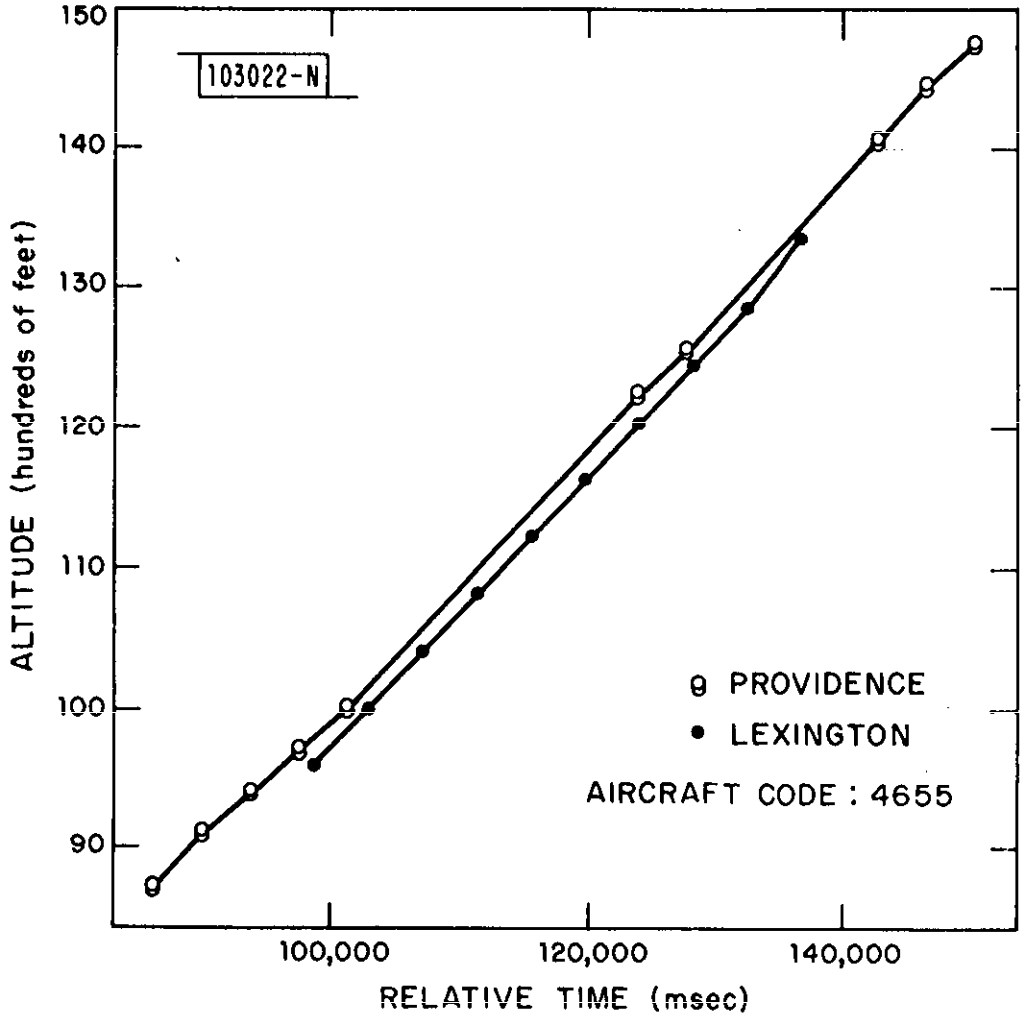

Fig. C-2. Example of time base offset between sensors.

APPENDIX D

MATHEMATICAL OVERVIEW

A. Introduction

This Appendix includes background information relevant to topics included in the main body of the report. The level of coverage is not intended to be rigorous and the reader interested in additional detail should consult references listed in the bibliography.

B. Maximum Likelihood Bias Estimator

The discrepancy or residual in apparent aircraft position as reported by two sensors at some time t_i is modelled as a two-element Gaussian random vector Δ_i,

$$\Delta_i = \begin{pmatrix} X \\ Y \end{pmatrix}_i \tag{D1}$$

where X is the geographic north-south component of the residual and Y is the east-west component.

The probability density function for Δ_i can be written as:

$$P(\Delta_i) = \frac{1}{|C_i|^{1/2}\, 2\pi}\, e^{-\frac{1}{2}\,(\Delta_i^T\, C_i^{-1}\, \Delta_i)} \tag{D2}$$

where Δ_i^T is the transpose of Δ_i and C_i^{-1} is the inverse of the covariance matrix of the residuals. This matrix will be developed below on the assumption that the bias values are known and that the residuals arise exclusively from measurement error in both sensors.

For N independent observations of the aircraft, the joint probability density function $P(\Delta_1, \Delta_2, \ldots \Delta_N)$ is given by:

$$P(\Delta_1, \Delta_2, \ldots \Delta_N) = \frac{1}{(2\pi)^N \prod_{i=1}^{N} |C_i|^{1/2}}\, e^{-\frac{1}{2}\sum_{i=1}^{N} (\Delta_i^T\ C_i^{-1}\ \Delta_i)} \tag{D3}$$

The maximum likelihood choice of bias parameters is based on the idea that the underlying system should be the one which makes the observed set of Δ_i much more likely than any others. Thus, one would expect the best estimate of the bias parameters to be that which maximizes the joint probability density function. Because of the negative exponent, this amounts to minimizing the function:

$$S = \sum_{i=1}^{N} (\Delta_i^T C_i^{-1} \Delta_i) \tag{D4}$$

The covariance matrix of the residuals will be developed by first considering the measurement error covariance matrix from one of the two radars. We would like this covariance to be expressed in the common Cartesian system into which all local measurements are transformed.

From the geometry of Figure B-1 it follows that the measurement can be written in Cartesian coordinates as:

$$x = R \sin \theta$$
$$y = R \cos \theta$$

It will be assumed that measurement errors in R and θ are each zero mean and independent and have a covaraince matrix,

$$C_{R\theta} = \begin{pmatrix} \sigma_R^2 & 0 \\ 0 & \sigma_\theta^2 \end{pmatrix}$$

Now, by the principle of the propagation of covariances, we can write,

$$C_{xy} = F \, C_{R\theta} \, F^T$$

where:

$$F = \begin{pmatrix} \frac{\partial x}{\partial R} & \frac{\partial x}{\partial \theta} \\ \frac{\partial y}{\partial R} & \frac{\partial y}{\partial \theta} \end{pmatrix}$$

Upon performing the indicated differentiations and matrix multiplications, the desired measurement covariance matrix for one sensor can be written as:

$$C_{xy} = \begin{pmatrix} \sin^2 \theta_i \, \sigma_R^2 + R_i^2 \cos^2 \theta_i \, \sigma_\theta^2 & \sin \theta_i \cos \theta_i \, (\sigma_R^2 - R_i^2 \, \sigma_\theta^2) \\ \sin \theta_i \cos \theta_i \, (\sigma_R^2 - R_i^2 \, \sigma_\theta^2) & \cos^2 \theta_i \, \sigma_R^2 + R_i^2 \sin^2 \theta_i \, \sigma_\theta^2 \end{pmatrix}$$

Residuals in the x and y directions can be simply expressed in terms of the latitude and longitude (ϕ, λ) of the aircraft's position. Specifically,

$$x = E \cos \phi_2 \, (\lambda_2 - \lambda_1)$$

$$y = E \, (\phi_2 - \phi_1)$$

where E is the mean radius of the referenced earth ellipsoid and the subscripts on ϕ and λ identify the reporting sensor. The factor $\cos \phi_2$ in the expression for x was arbitrarily selected as a scaling factor; $\cos \phi_1$ could have been used instead.

Recall that Δ_i is calculated from the difference between two observations. By taking these to be independent, the covariance of the residuals is then just the sum of the covariances of the measurement errors from the two sensors. If this sum matrix is written as:

$$C_i = C_{xy}^{\text{sensor 1}} + C_{xy}^{\text{sensor 2}}$$

or

$$C_i = \begin{pmatrix} b_{11} & b_{12} \\ b_{12} & B_{22} \end{pmatrix}$$

then the function S to be minimized can be expressed as:

$$S = \frac{1}{(b_{11} \, b_{22} - b_{12}^2)} \, (b_{22} \, x^2 - 2 \, b_{12} \, xy + b_{11} \, y^2)$$

It can be shown by substitution that S is the sum of the squares of the scaled projections of the vector Δ_i on the major and minor axes of the error ellipse. The scale factors are the error ellipse axes themselves. Thus, the length of a difference vector alone is not as important in determining the biases as is the length and orientation with respect to the combined error ellipse at the aircraft position.

Presented in Figure D-1 is a geometrical interpretation of the term $\Delta_i^T C_i^{-1} \Delta_i$ at the i^{th} "superpoint" sample time. As the aircraft changes position with respect to the two sensors, the effective weighting of a residual vector of a given length varies accordingly.

C. Variance of the Bias Estimate

Analysis of the error associated with the bias estimates considered in this report would be quite complex owing to the non-linear character of the problem. It is, however, instructive to consider instead a simpler problem:

Given a set of observations x_i, y_i $i = 1,N$, and an assumed function

$$y(x) = \sum_{j=0}^{K} a_j Q_j(x)$$

Find the parameters a_j such that the quantity

$$X^2 = \sum_{i=1}^{N} \frac{1}{\sigma_i^2} \{y_i - y(x_i)\}^2 \qquad \text{is minimized.}$$

$Q_j(x)$ is typically a polynomial in x while σ_i^2 is the sample variance of the y_i's.

Required in the development of the variance of the parameter estimates is the K by K symmetric matrix H whose elements $h_{j\ell}$ are:

$$h_{j\ell} = \frac{1}{2} \frac{\partial^2 X^2}{\partial a_j \partial a_\ell}$$

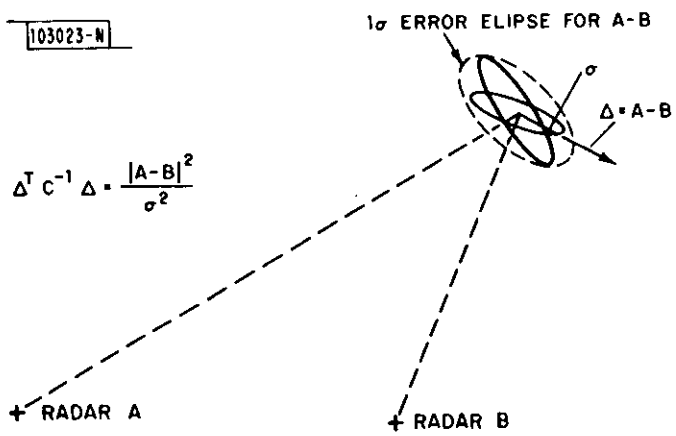

Fig. D-1. Geometrical interpretation of $\Delta^T C^{-1} \Delta$.

This matrix is referred to as the Hessian matrix and, more descriptively, as the curvature matrix because of its relationship to the curvature of X^2 in parameter space.

It can be shown that

$$a_j = \sum_{\ell=0}^{K} \{ \varepsilon_{j\ell} \sum_{i=1}^{N} (\frac{1}{\sigma_i^2} y_i Q_\ell (x_i))\}$$

where $\varepsilon_{j\ell}$ is an element of the matrix E where

$$E = H^{-1}$$

The uncertainty in the parameters can be estimated from:

$$\sigma_{a_j}^2 = \sum_{i=1}^{N} \sigma_i^2 (\frac{\partial a_j}{\partial y_i})^2$$

The derivative in the summation can be expressed as:

$$\frac{\partial a_j}{\partial y_i} = \sum_{\ell=0}^{K} (\frac{\varepsilon_{j\ell}}{\sigma_i^2}) Q_\ell (x_i)$$

Substituting and rearranging, the variance of the parameter estimate becomes:

$$\sigma_{a_j}^2 = \varepsilon_{jj}$$

Because of this relationship, the matrix $E = (\varepsilon_{jk})$ is called the error matrix.

D. Combining Biases from Two or More Aircraft

Having obtained an estimate of a bias a_m from the m^{th} aircraft and its associated variance $\sigma_{a_m}^2$, it will now be shown how estimates from M different aircraft should be combined to obtain the best possible composite estimate $\hat{a}$. Assuming Gaussian probability again, we maximize the probability of getting the observed M estimates by minimizing the associated probability density function.

The exponent of this function can be shown to be:

$$-\frac{1}{2}\sum_{m=1}^{M}\frac{(a_m - \hat{a})^2}{\sigma_{a_m}^2}$$

and thus the task at hand is to minimize by taking $\partial/\partial a_m$ and setting equal to zero.

$$-\frac{1}{2}\frac{\partial}{\partial a_m}\left(\sum_{m=1}^{M}\frac{(a_m - \hat{a})^2}{\sigma_{a_m}^2}\right) = 0$$

simplifying

$$\sum_{m=1}^{M}\frac{(a_m - \hat{a})}{\sigma_{a_m}^2} = 0$$

solving for $\hat{a}$:

$$\hat{a} = \sum_{m=1}^{M}\frac{a_m}{\sigma_{a_m}^2} \Big/ \sum_{m=1}^{M}\frac{1}{\sigma_{a_m}^2}$$

Thus, the composite bias estimate is a weighted mean and its variance is given by

$$\sigma_{\hat{a}}^2 = \frac{1}{\sum_{m=1}^{M}\left(\frac{1}{\sigma_{a_m}^2}\right)}$$

E. Mean and Variance for S

Given the statistic S

$$S = \frac{1}{\nu}\sum_{i=1}^{N}\frac{x_i^2}{\sigma_x^2}$$

where x_i is assumed to be a zero mean Gaussian variable and x_j, x_k for $j \neq k$, are independent. Also assumed is that the variances are equal, i.e., $\sigma_{x_k}^2 = \sigma_x^2$ for all K. It is well known that S has a chi-square distribution with ν degrees of freedom.

Expressions for the mean and variance of S will now be developed.

Mean

$$\bar{S} = E[S] = E\left[\frac{1}{\nu}\sum_{i=1}^{N}\frac{x_i^2}{\sigma_x^2}\right]$$

$$= \frac{1}{\nu\,\sigma_x^2} E\left[\sum_{i=1}^{N} x_i^2\right]$$

$$= \frac{N\,\sigma_x^2}{\nu\,\sigma_x^2} = \frac{N}{\nu}$$

Variance

$$Var(S) = E\left[(S - E[S])^2\right]$$

$$= E\left[\left(\frac{1}{\nu}\sum_{i=1}^{N}\frac{x_i^2}{\sigma_x^2} - E[S]\right)^2\right]$$

Substituting for the mean and expanding:

$$Var(S) = E\left[\left(\frac{1}{\nu}\sum_{j=1}^{N}\frac{x_j^2}{\sigma_x^2}\right)\left(\frac{1}{\nu}\sum_{K=1}^{N}\frac{x_K^2}{\sigma_x^2}\right) - \frac{2}{\nu}\left(\sum_{i=1}^{N}\frac{x_i^2}{\sigma_x^2}\right)\frac{N}{\nu} + \left(\frac{N}{\nu}\right)^2\right]$$

By carrying through the expectancy operation for each term,

$$= E\left[\left(\frac{1}{\nu}\sum_{j=1}^{N}\frac{x_j^2}{\sigma_x^2}\right)\left(\frac{1}{\nu}\sum_{K=1}^{N}\frac{x_K^2}{\sigma_x^2}\right)\right] - E\left[\frac{2N}{\nu^2}\sum\frac{x_K^2}{\sigma_x^2}\right] + E\left[\frac{N^2}{\nu^2}\right]$$

The middle term becomes:

$$-\frac{2}{\nu}\left(\frac{N\sigma_x^2}{\sigma_x^2}\right)\frac{N}{\nu} = -\frac{2N^2}{\nu^2}$$

and, thus, the second and last terms combine to:

$$\frac{-N^2}{\nu^2}$$

What remains then is to reduce the first term; the expectancy of the product of two summations.

Factoring out the σ_x^2 from the denominator in the summation, the first term can be written as:

$$\frac{1}{\nu^2 \sigma_x^2} \; E\left[\left(\sum_{j=1}^{N} x_j^2\right)\left(\sum_{K=1}^{N} x_K^2\right)\right]$$

The product of the summations includes N^2 terms of which N are of the form:

$$x_j^4 \qquad j = 1,N$$

and it can be shown by Gaussian moment factoring that

$$E[x^4] = 3\,\sigma_x^4$$

The remaining $N^2 - N$ terms of the product are of the form

$$x_i^2\, x_j^2 \qquad i \neq j$$

and since the x_i's are independent and have equal variances and zero mean

$$E\left[x_i^2\, x_j^2\right] = E\left[x_i^2\right]\; E\left[x_j^2\right] = \sigma_x^2\, \sigma_x^2 = \sigma_x^4$$

Thus, the term above involving the product of the summations becomes:

$$\frac{1}{\nu^2\, \sigma_x^4}\left(3\,N\,\sigma_x^4 + (N^2 - N)\,\sigma_x^4\right) = \frac{N^2 + 2\,N}{\nu^2}$$

and, finally, the variance of S can be obtained by combining results and

$$\mathrm{Var}(S) = \frac{N^2 + 2\,N}{\nu^2} - \frac{N^2}{\nu^2}$$

$$= \frac{2\,N}{\nu^2}$$

For the problem considered in this report, ν is the number of degrees of freedom

$$\nu = N - L - 1$$

where L is the number of bias components present and N is twice the number of "superpoints" employed in the estimation (one for each of the x and y residuals).

For N large, the mean of S approaches 1 while the variance approaches 2/N.

UNCLASSIFIED

SECURITY CLASSIFICATION OF THIS PAGE *(When Data Entered)*

REPORT DOCUMENTATION PAGE

READ INSTRUCTIONS BEFORE COMPLETING FORM

1. REPORT NUMBER: ESD-TR-80-169
2. GOVT ACCESSION NO.:
3. RECIPIENT'S CATALOG NUMBER:

4. TITLE *(and Subtitle)*: Registration Errors in a Netted Air Surveillance System

5. TYPE OF REPORT & PERIOD COVERED: Technical Note

6. PERFORMING ORG. REPORT NUMBER: Technical Note 1980-40

7. AUTHOR(s): William L. Fischer, Alan G. Cameron, Charles E. Muehe

8. CONTRACT OR GRANT NUMBER(s): F19628-80-C-0002

9. PERFORMING ORGANIZATION NAME AND ADDRESS:
Lincoln Laboratory, M.I.T.
P.O. Box 73
Lexington, MA 02173

10. PROGRAM ELEMENT, PROJECT, TASK AREA & WORK UNIT NUMBERS: Program Element No. 62702F, Project No. 4506

11. CONTROLLING OFFICE NAME AND ADDRESS:
Air Force Systems Command, USAF
Andrews AFB
Washington, DC 20331

U.S. Army Communications Research and Development Command
DRDCO-SEI-V
Ft. Monmouth, NJ 07703

12. REPORT DATE: 2 September 1980

13. NUMBER OF PAGES: 84

14. MONITORING AGENCY NAME & ADDRESS *(if different from Controlling Office)*:
Electronic Systems Division
Hanscom AFB
Bedford, MA 01731

15. SECURITY CLASS. *(of this report)*: Unclassified

15a. DECLASSIFICATION DOWNGRADING SCHEDULE:

16. DISTRIBUTION STATEMENT *(of this Report)*:
Approved for public release; distribution unlimited.

17. DISTRIBUTION STATEMENT *(of the abstract entered in Block 20, if different from Report)*:

18. SUPPLEMENTARY NOTES:
None

19. KEY WORDS *(Continue on reverse side if necessary and identify by block number)*:
netted surveillance radar
integrated air surveillance system
multisensors
automated sensor registration

20. ABSTRACT *(Continue on reverse side if necessary and identify by block number)*:

Today's tactical military air surveillance radars generally operate in a stand-alone configuration. The many performance improvements that result when data from multiple radars of this type are merged have made such netted operations an attractive goal for many years. A major obstacle to achieving this goal has traditionally been the difficulty associated with the registration of multisensor data, the expression of the data in a common coordinate system free from errors due to site uncertainty, antenna orientation, and improper alignment.

This report presents the results of a modest effort to develop a self-registration procedure by which multiple radar sensors operating in consort each calculate the errors in their data by comparing it with data from the remainder of the system and then uses the information to upgrade performance. The technique has been tested with experimental data and appears quite capable of improving system performance, measured in terms of residual inter-site bias errors, by almost a factor of one hundred.

DD FORM 1 JAN 73 1473 EDITION OF 1 NOV 65 IS OBSOLETE

UNCLASSIFIED

SECURITY CLASSIFICATION OF THIS PAGE *(When Data Entered)*